

# Review

<https://doi.org/10.48130/bchax-0025-0006>

## Animal manure biochar for the removal of hazardous pollutants from wastewater

Sangyoon Lee<sup>1</sup>, Minyoung Kim<sup>1</sup>, Gyeongnam Park<sup>1</sup>, Sungyup Jung<sup>2</sup> and Eilhann E. Kwon<sup>1\*</sup>

Received: 11 June 2025

Revised: 1 September 2025

Accepted: 16 September 2025

Published online: 30 September 2025

### Abstract

The improper management of animal manure, a major byproduct of the livestock industry, presents significant environmental challenges. Thermochemical conversion, particularly pyrolysis, offers a viable pathway for valorising manure into biochar, a carbon-rich material with demonstrated potential for wastewater remediation. This review explores the use of manure-derived biochar as an effective adsorbent for various hazardous organic and inorganic contaminants, including dyes, antibiotics, and heavy metals. Adsorption mechanisms are attributed to physical (e.g., pore filling and van der Waals forces) and chemical interactions (e.g., electrostatic attraction, hydrogen bonding, ion exchange, and  $\pi$ - $\pi$  electron donor-acceptor interactions). Owing to the abundance of mineral phases (e.g., carbonate, phosphate) and reactive functional groups (e.g., -COOH, -OH), manure-derived biochars support diverse adsorption mechanisms, including electrostatic interactions,  $\pi$ - $\pi$  electron donor-acceptor (EDA) interactions, hydrogen bonding, ion exchange, surface complexation, and mineral precipitation. This review specifically evaluates the major adsorption mechanisms of various pollutants on manure-derived biochar, providing pollutant-specific guidance for biochar production. The effects of the pyrolysis conditions, manure type, surface modification strategies, and intrinsic mineral composition on the adsorption performance are discussed. The intrinsic characteristics of biochar enable reliable adsorption performance for dyes and heavy metals [such as Pb(II), Cu(II), and Cd(II)] via simple pyrolysis, whereas antibiotic removal requires tailored biochar production because of the distinct physicochemical properties of each antibiotic. Finally, this review addresses the cost-effectiveness, regeneration strategies, and key practical factors influencing large-scale adoption in wastewater treatment and outlines future directions for integrating manure-derived biochar into real-world manure management systems.

**Keywords:** Waste valorisation, Animal manure, Pyrolysis, Biochar, Wastewater treatment, Adsorption

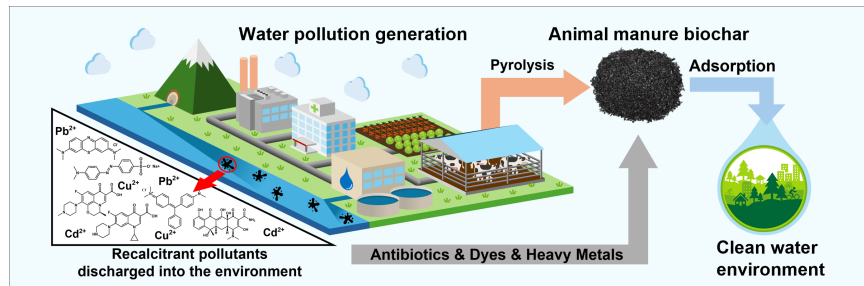
### Highlights

- Animal manure biochar as an adsorbent for wastewater treatment was reviewed.
- Heteroatoms and surface functional groups enhance biochar's adsorption capacity.
- Adsorption mechanisms for organic pollutants and heavy metals were explored.
- The technical advantages and limitations of animal manure biochar were discussed.

\* Correspondence: Eilhann E. Kwon ([ek2148@hanyang.ac.kr](mailto:ek2148@hanyang.ac.kr))

Full list of author information is available at the end of the article.

## Graphical abstract



## Introduction

Water is an essential resource for humanity because it is fundamental to sustaining life, supporting agriculture, and maintaining public health<sup>[1]</sup>. Economic growth, technological advancement, and urbanisation have further driven the expansion of water-intensive industries, such as power generation, textiles, chemicals, and food processing, thereby intensifying the demand for water<sup>[2,3]</sup>. As water consumption has increased, the generation of wastewater containing chemicals, heavy metals, fertilisers, pharmaceuticals, and other contaminants from various sectors has also increased<sup>[4]</sup>. Without proper treatment prior to discharge, this wastewater pollutes the surrounding water bodies, including rivers, groundwater, and oceans, leading to severe impacts on ecosystems and public health<sup>[5]</sup>. Consequently, the implementation of an effective water treatment strategy is imperative for securing clean water resources and protecting the surrounding ecosystems<sup>[6]</sup>.

Conventional wastewater treatment plants (WWTPs), which are effective in removing organic matter and suspended solids through primary (physical) and secondary (biological) processes, face limitations in eliminating specific industrial pollutants<sup>[4]</sup>. Recalcitrant organic compounds (e.g., dyes, antibiotics, and pesticides) exhibit complex molecular structures that resist biodegradation during conventional biological treatment<sup>[5]</sup>. Similarly, heavy metals (e.g., Pb, Cu, and Cd) cannot be degraded. Therefore, as illustrated in Fig. 1, the development and implementation of advanced treatment technologies, including membrane filtration, precipitation, coagulation-flocculation, electrochemical treatment, ion exchange, and adsorption, as tertiary processes in WWTPs have received significant attention for the removal of recalcitrant organic pollutants and heavy metals<sup>[6]</sup>. Among them, adsorption has emerged as a versatile and cost-effective method for removing diverse heavy metals and organic pollutants and can be tailored with various adsorbents for specific contaminants<sup>[7]</sup>. Furthermore, adsorption can remove trace-level and nonbiodegradable pollutants<sup>[8]</sup>. Notably, adsorbents

such as activated carbon, biochar, clay minerals, and engineered nanomaterials offer high surface areas and functional groups, enabling the immobilisation of pollutants through physical or chemical binding<sup>[9–11]</sup>. Among these, biochar has emerged as an advantageous adsorbent because of its cost-effectiveness and commitment to environmental sustainability. Biochar is a carbon-rich material typically generated through the thermal decomposition of biomass in an oxygen-free environment, known as pyrolysis<sup>[12]</sup>. Furthermore, the physicochemical properties of biochar that enhance its efficacy in pollutant removal can be optimised through careful feedstock selection and the regulation of pyrolysis conditions.

To utilise biochar as a sorptive material, a constant supply of raw feedstock at low cost must be ensured<sup>[13]</sup>. Among biomass sources, animal manure represents a promising and economically viable option owing to its high availability as a stockbreeding byproduct. Animal manure is generated during the massive breeding of livestock globally because of constant population growth and meat consumption<sup>[14]</sup>. This abundance enables large-scale and sustainable use of biochar in wastewater treatment applications<sup>[15]</sup>. Additionally, animal manure is often costly to manage and poses a risk of environmental pollution and pathogen transmission<sup>[16]</sup>. Therefore, using animal manure as biochar feedstock contributes to reducing waste management burdens while transforming problematic materials into valuable resources.

Animal manure biochar has distinct physicochemical advantages that enhance its efficacy as an adsorbent. Compared with lignocellulosic residues, animal manure is characterised by higher concentrations of N, P, and inorganic elements such as Ca, K, and Mg, which originate from undigested feed and bedding materials<sup>[17]</sup>. These components impart unique physicochemical properties to the resulting biochar, including enhanced surface functionality, ion exchange capacity, and mineral-rich phases (e.g., carbonates and phosphates)<sup>[18]</sup>. These features facilitate physical (hydrophobic interactions, van der Waals forces, hydrogen bonding, and pore-filling) and chemical (electrostatic attraction,  $\pi$ - $\pi$  electron

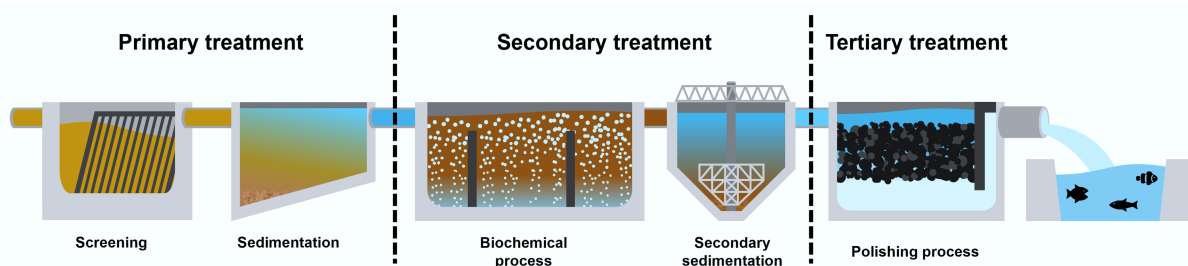


**Fig. 1** Schematic diagram of a wastewater treatment plant.

donor–acceptor [EDA] interactions, ion exchange, precipitation, and surface complexation) interactions, enabling the effective adsorption of various pollutants, including dyes, pharmaceutical residues, and heavy metals<sup>[19,20]</sup>. Despite these advantages, comprehensive studies on the utilisation of animal manure biochar have rarely been reported. This review provides a comprehensive overview of the production, activation, and application of animal manure biochar for the removal of hazardous pollutants (dyes, antibiotics, and heavy metals) from wastewater. It offers practical insights into how the pyrolysis conditions, manure type, surface modifications, and intrinsic mineral composition influence the adsorption performance. Conclusively, the dominant adsorption mechanisms are elucidated to inform pollutant-specific strategies for the effective application of manure-derived biochar. Additionally, this review highlights the economic feasibility, limitations, and future research directions necessary to advance the practical use of manure biochar in wastewater treatment applications.

## Production of animal manure wastes

With rapid population growth and the need for protein consumption, the global demand for meat has increased significantly in recent decades. According to the Organization for Economic Co-operation and Development statistics, global meat consumption has increased from 227 Mt in 2000 to 324 Mt in 2019 and is expected to increase by another 11% by 2029<sup>[21]</sup>. The continuous increase in meat consumption has resulted in an increase in the animal population and manure. Figure 2 illustrates the animal populations and manure production in representative countries on six continents in 2019. The total population of animals raised is highest in China, followed by the

USA, Brazil, France, Australia, and Ethiopia (Fig. 2a). Despite its numerical dominance, the generation of animal manure in Brazil was higher than that in China (Fig. 2b). The majority of global animal manure production is attributed to cattle and sheep, which contribute over 80% of the total output (Fig. 2b). This is because manure generation is closely correlated with the animal's weight.

For large-scale animal production, animals are bred in facilities designed to maximise the population density for intensive farming. This high-density practice influences the properties of the resulting manure. The manure generated in such systems is not solely in solid form; it is typically produced as a slurry owing to its simultaneous generation with urine<sup>[23]</sup>. Additionally, it contains a complex mixture of lignocellulosic biomass, including undigested feed (crops) and bedding materials (grass and straw)<sup>[24]</sup>. Manure produced in livestock facilities comprises animal excreta and organic biomass<sup>[25]</sup>. Table 1 summarises the proximate composition and organic and inorganic contents of animal manure in comparison with those of representative crop residues.

As summarised in Table 1, animal manure contains higher levels of N, P, and inorganic (Ca, K, Mg, Na, Fe, Al, and Si) components than wheat or rice straw. These components originate from the undigested residues of essential nutrients supplemented in the feed to support the animals' optimal growth and productivity<sup>[26,27]</sup>. Given that elements such as N, P, and inorganic components are essential for all living organisms, animal manure has potential as a nutrient source in agriculture to enhance soil fertility<sup>[28]</sup>. Despite the abundance of nutrients, the direct application of animal manure is limited by sanitation concerns, including the potential transmission of pathogens and toxicants<sup>[16]</sup>. Thermochemical conversion has gained attention as a promising valorisation pathway, enabling the

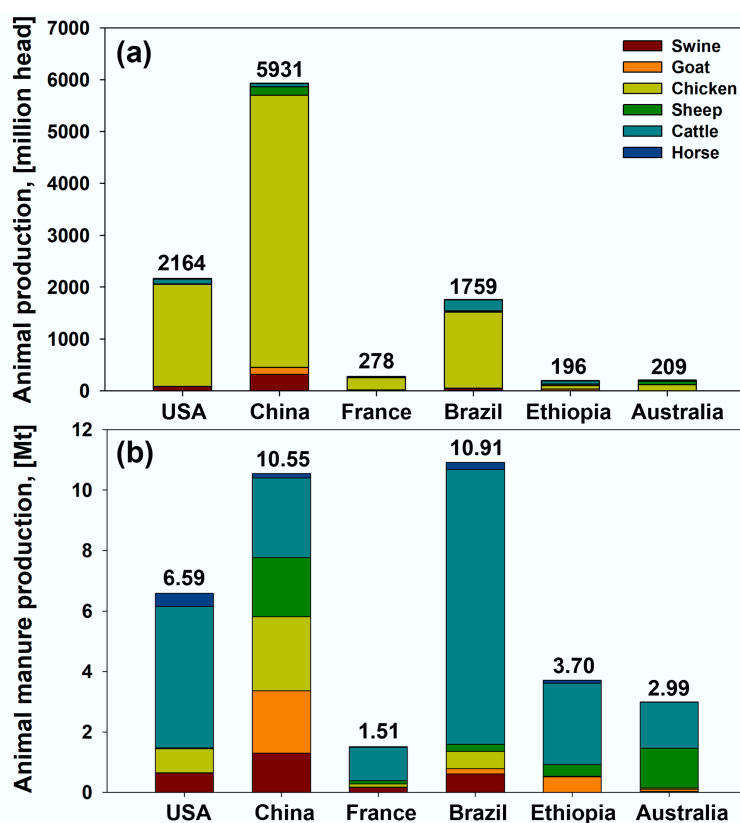


**Fig. 2** (a) Annual animal (swine, goat, chicken, sheep, cattle, and horse) populations and (b) their manure production in the USA, China, France, Brazil, Ethiopia, and Australia (2019)<sup>[22]</sup>.

**Table 1** The proximate, organic, and inorganic contents of animal manure with reference to representative crop residues

Parameter	Lignocellulosic biomass (wt.%)		Animal manure waste (wt.%)				
	Wheat straw	Rice straw	Swine manure	Goat manure	Chicken manure	Sheep manure	Cattle manure
Proximate analysis (dry sample basis)							
Moisture	1.8–6.3	Not determined	4.4–13.6	6.0–8.7	5.6–10.0	8	1.6
Volatile matter	61.0–83.3	65.5–76.1	52.1–69.4	62.7–69.5	61.3–74.6	59.98	60.9–73.5
Fixed carbon	10.3–29.5	14.3–19.2	10.5–22.8	4.5–12.9	6.2–22.8	12.79	10.3–16.3
Ash	1.4–17.6	9.6–19.6	10.2–35.8	17.3–29.0	11.6–28.1	16.1–19.2	10.2–31.9
Ultimate analysis (dry sample basis)							
C	41.0–46.7	30.5–40.4	37.7–52.2	26.5–40.1	28.2–43.9	41.5–42.4	34.4–42.4
H	2.3–6.0	3.9–5.6	3.8–7.8	3.7–5.9	3.5–6.5	5.2–6.1	4.9–5.9
O	40.6–51.4	39.6–47.3	28.9–44.2	37.4–41.2	32.8–35.5	31.4–32.1	28.7–42.3
N	0.1–0.8	0.4–1.4	1.1–5.8	1.5–2.0	3.7–8.1	2.1–2.9	1.9–2.3
S	0.1–0.2	0.6 >	0.2–0.7	0.03	0.2–1.5	0.4–0.6	0.3–0.6
Inorganic material (dry sample basis)							
P	0.1 >	0.5–0.7	1.6–4.9	1.0–1.9	0.4–2.4	0.4–1.4	0.2–1.5
Ca	0.3–0.4	0.3–0.6	0.2–5.0	2.1–3.9	1.8–5.9	0.8–5.11	0.1–8.3
K	1.8–2.6	1.5–2.3	0.4–7.8	1.6–3.4	0.7–3.1	1.9–3.3	0.9–6.2
Mg	0.1–0.2	0.2–0.5	0.5–2.0	0.8–1.8	0.3–0.7	0.5–0.7	0.1–1.1
Na	0.2–0.3	0.3 >	0.1–0.4	–	0.4–0.9	0.4	0.2–0.4
Fe	0.1 >	0.1 >	0.1–1.3	0.2	0.1 >	–	0.3–0.4
Al	0.1 >	0.3 >	0.1–0.4	0.2	0.1 >	–	1.6
Si	2.4	5.0–13.9	0.1 >	–	–	–	–

recovery of valuable products such as syngas, bio-crude, and bio-char from organic matter while simultaneously stabilising hazardous substances<sup>[29]</sup>. In particular, the abundance of heteroatoms and metals in animal manure makes biochar an efficient sorptive material<sup>[30]</sup>. These elements alter the electron density of the C matrix in biochar, enhancing its adsorption performance.

## Biochar production from animal manure

Biochar is a C-rich porous material characterised by a high surface area, well-developed porosity, and surface functional groups<sup>[31]</sup>. Because of its physicochemical properties, it has been widely applied as an adsorbent for the removal of pollutants from wastewater. Therefore, it is essential to develop appropriate surface properties to utilise biochar effectively as an adsorbent. Biochar is typically produced through the thermochemical decomposition of biomass under oxygen-free conditions, which is known as pyrolysis<sup>[32]</sup>. During pyrolysis, biochar is formed via primary and secondary thermal cracking processes. Under primary cracking, rising temperatures break the covalent bonds in biopolymers, leading to the release of volatile matter (VM; gaseous and liquid pyrolysates) and the formation of a solid carbonaceous residue (biochar)<sup>[33]</sup>. In secondary reactions, the released VM undergoes further thermal decomposition and reduction (repolymerisation), resulting in additional C-rich solid residues, commonly referred to as coke<sup>[34]</sup>. The surface properties and yield of the resulting biochar are influenced by the extent of these pyrolytic reactions, which, in turn, are affected by operational parameters such as reaction temperature, heating rate, and residence time<sup>[35]</sup>. Depending on these parameters, the pyrolysis is typically classified as flash, fast, or slow.

## Pyrolysis

Flash pyrolysis is generally conducted at high temperatures (400–1,200 °C) with rapid heating rates (> 1,000 °C min<sup>-1</sup>) and a reaction time of < 2 s<sup>[36–38]</sup>. Fast pyrolysis is conducted at high temperatures (400–1,000 °C), fast heating rates (300–1,200 °C min<sup>-1</sup>), and short residence times (0.5–10 s)<sup>[36,37]</sup>. Flash and fast pyrolysis processes typically do not produce biochar because they tend to yield VM (Table 2). This is attributed to the high heating rates and reaction temperatures, which facilitate primary decomposition reactions while simultaneously inhibiting secondary reactions such as the repolymerisation of volatiles into coke. In contrast, slow pyrolysis is conducted at lower temperatures (300–900 °C), slower heating rates (5–60 °C min<sup>-1</sup>), and longer residence times (5–360 min)<sup>[36,39]</sup>. The slow heating rate naturally results in a prolonged residence time at low reaction temperatures, facilitating the secondary reaction of the bio-crude product and promoting the formation of coke through repolymerisation<sup>[40]</sup>. Therefore, slow pyrolysis is preferred for producing biochar owing to its high yield.

## Activation of animal manure biochar

The adsorption performance of biochar is influenced by its surface properties, including specific surface area, pore structure, and reactive functional groups<sup>[31]</sup>. However, biochar produced through conventional pyrolysis often exhibits limited surface development as a result of pore blockage or collapse during carbonisation, which restricts its adsorption capacity<sup>[41]</sup>. Additionally, elevated pyrolysis temperatures destroy or alter the surface functional groups, further reducing its adsorption potential<sup>[42]</sup>. In this context, activating biochar can enhance its surface properties by generating porosity and introducing various functional groups before its application as an adsorbent<sup>[42]</sup>. Various

**Table 2** Operation conditions, biochar production yields, and target products of different thermo-chemical processes

Process	Temperature (°C)	Heating rate (°C min <sup>-1</sup> )	Reaction medium	Residence time	Biochar yield (wt.%)	Target product
Flash pyrolysis	400–1,200	> 1,000	Inert gas (N <sub>2</sub> , Ar, etc.)	< 2 s	10–20	Pyrolytic oil
Fast pyrolysis	400–1,000	300–1,200		0.5–10 s	15–35	Pyrolytic oil
Slow pyrolysis	300–900	5–60		5 min–12 h	25–50	Biochar



activation strategies have been explored, including physical and chemical treatments, and metal impregnation.

### Physical activation

Physical activation involves activating biochar at elevated temperatures with or without the presence of oxidising agents such as air, steam, CO<sub>2</sub>, hydrogen peroxide (H<sub>2</sub>O<sub>2</sub>), or their mixtures. The CO<sub>2</sub> and H<sub>2</sub> gases evolved during pyrolysis in the presence of oxidising agents contribute to the activation of the biochar's surface. This activation promotes the development of micropores and mesopores, resulting in a wider pore size distribution<sup>[43]</sup>. It should be noted that CO<sub>2</sub> activation can effectively enhance the formation of micropores through controlled gas–solid reactions, while steam activation primarily increases the surface area and mesopore volume<sup>[44]</sup>. In addition, physical activation can introduce oxygen (O)-containing functional groups, such as phenolic and carboxylic groups, onto the biochar's surface<sup>[45]</sup>. For instance, H<sub>2</sub>O<sub>2</sub> treatment expands the micropores of biochar and increases the abundance of O-containing functional groups, primarily carbonyl (C=O) and hydroxyl (–OH) groups<sup>[46]</sup>.

### Chemical activation

The chemical activation of biochar significantly enhances the adsorptive and structural properties of raw biochar. It is generally performed by mixing biochar with activating agents, such as acids (e.g., H<sub>2</sub>SO<sub>4</sub> and HNO<sub>3</sub>) and alkalis (e.g., KOH and NaOH)<sup>[47]</sup>. Chemical activation typically involves mixing biochar with chemical agents, followed by thermal treatment. This process dehydrates the biochar and increases carbonization, thereby promoting the formation of pores, including nanopores and functional groups<sup>[48]</sup>. After activation, the residual chemicals are removed by washing with deionised water, and the surface pH may be adjusted using acid or basic solutions<sup>[42]</sup>. The physicochemical properties of chemically activated biochar are affected by the chemical reagent<sup>[49]</sup>.

Acid activation enhances the surface properties of biochar by introducing additional O-containing functional groups, while improving the surface area. Acidic agents facilitate the formation of carbonyl and hydroxyl groups on the biochar's surface by oxidising aromatic rings and aliphatic chains<sup>[50]</sup>. In addition, acid hydrolysis induces dehydration and degradation, leading to the formation of ketones and other carbonyl-containing functional groups<sup>[51]</sup>. For instance, Wang et al.<sup>[52]</sup> demonstrated that HNO<sub>3</sub> activation effectively improved the specific surface area and enriched the presence of O-containing functional groups, such as carboxyl and carbonyl groups, in swine manure biochar.

Activation with alkaline agents improves the surface properties of biochar by introducing O-containing functional groups and imparting basicity to its surface<sup>[53]</sup>. These modifications provide ionic exchange sites that facilitate the removal of pollutants, including anionic species and heavy metals, from wastewater<sup>[54]</sup>. For example, KOH activation promotes the formation of functional groups such as hydroxyl (R–OH), carbonyl (C=O), alkene (C=C), and aromatic structures<sup>[55]</sup>. In addition, Wang et al.<sup>[52]</sup> reported that KOH-modified swine manure biochar exhibited a significantly higher surface area than pristine biochar.

### Metal-impregnated biochar

Metal and metal oxide impregnation promotes the development of biochar's properties such as surface area<sup>[56]</sup> and functional groups, thereby improving its adsorption capacity<sup>[57,58]</sup>. Metal impregnation is performed using a dissolved metal solution containing metal salts (e.g., MgCl<sub>2</sub>, AlCl<sub>3</sub>, and FeCl<sub>3</sub>) and/or metal oxides (e.g., MnO, ZnO, and FeO). This process is typically achieved by mixing the precursors with biomass before pyrolysis for in-situ activation, or by impregnating the produced biochar followed by thermal treatment for post-pyrolysis

activation<sup>[47]</sup>. Among metal salts/oxides, iron impregnation has gained significant interest owing to its nontoxic nature, stable adsorption performance, and ease of separation from wastewater using an external magnetic field<sup>[59]</sup>. Notably, Fe-impregnated biochar exhibits particularly stable adsorption behaviour for the removal of heavy metals. This effectiveness is attributed to the chelation of Fe<sup>3+</sup> ions with surface functional groups, which facilitates the formation of metal oxides that are critical in the removal of heavy metal ions<sup>[60]</sup>.

### Comparison of modification methods

Balancing performance enhancement with practical viability, including operational convenience, cost, and technical feasibility, is essential when determining modification methods for manure-derived biochar. Physical modification of manure-derived biochar is technically convenient because of its simplicity, scalability, and minimal chemical requirements, making it suitable for large-scale applications. The key advantages include lower operational costs compared with chemical methods, reduced environmental risks from reagent use, and ease of integration into existing pyrolysis systems. However, physical modification generally requires higher activation temperatures and longer processing times, which increase energy consumption<sup>[61]</sup>, and its ability to introduce new functional groups is limited, often necessitating an additional chemical or metal impregnation step for targeted contaminant removal. Moreover, some methods, such as oxygen/air activation, can lead to uncontrolled carbon loss and random pore development. Overall, physical modification offers high technical feasibility and operational convenience but is less effective than chemical routes in tailoring the surface chemistry for specific applications.

Chemical modification of manure-derived biochar can substantially improve the surface functionality, porosity, and adsorption performance by introducing O-containing functional groups (e.g., –COOH, –OH, C=O) and altering the pore structures<sup>[62]</sup>. Acid treatments are effective in removing mineral impurities and enhancing the affinity for cationic pollutants, whereas alkaline treatments can dissolve ash, unblock pores, and increase adsorption sites for both metals and oxyanions<sup>[63]</sup>. These methods offer high-performance gains and allow adjustment of the surface chemistry, making them technically feasible for targeted pollutant removal. However, they require the use of chemical reagents, corrosion-resistant equipment, and substantial post-treatment washing to remove residual chemicals, which generates large volumes of wastewater and increases the operational costs<sup>[47]</sup>. Additional expenses stem from purchasing and storing chemical agents, as well as neutralising spent solutions. Because of these environmental and safety considerations, they demand greater caution than physical modification methods.

Metal modification of manure-derived biochar is achieved either by in situ impregnation of the feedstock before pyrolysis or post-pyrolysis impregnation. In situ methods integrate chemical loading and thermal activation into a single step, reducing handling and energy use, while post-pyrolysis methods offer better control over the metal's distribution at the cost of increased complexity and additional thermal treatment<sup>[47]</sup>. Key advantages include the ability to impart targeted functionalities, such as magnetic recovery using Fe-based biochars or improved oxyanion removal with Mg-, Al-, or Mn-modified biochars<sup>[60]</sup>. However, these methods' large-scale feasibility is constrained by potential reductions in surface area caused by pore blockage and the risk of corrosion from acidic solutions. In addition, the modification process generates metal-containing wastewater that demands dedicated post-treatment facilities, and ensuring uniform metal loading on the biochar requires greater operational expertise. Thus, while technically viable for high-value

applications in treatment facilities with an appropriate infrastructure, metal modification is generally less practical than simpler physical or alkaline activation methods.

In summary, physical modification is the most practical choice for large-scale, low-cost manure biochar production, offering simple integration, low environmental impact, and minimal operational hazards. Alkaline and acid treatments yield substantial performance improvements while requiring more advanced infrastructure and careful waste management. Metal modification provides high selectivity and additional functionalities for specific applications, but its implementation requires specialised expertise. Considering the advantages and disadvantages of each method, the optimal approach should be selected according to the specific end-use, the available technical capacity, and the balance between improved performance and operational feasibility.

## Generation of pollutants

### Organic pollutants

Conventional water treatment processes commonly use activated sludge because of its cost-effectiveness. Although this method efficiently removes most organic pollutants, recalcitrant compounds persist because of their resistance to microbial degradation<sup>[64]</sup>. Consequently, these pollutants are discharged into the surrounding environment, where they persist and accumulate over time. Among the recalcitrant organic pollutants, dyes and antibiotics are considered representative compounds because of their complex molecular structures, such as azo ( $-N=N-$ ) bonds and aromatic rings, which contribute to their inherent resistance to degradation<sup>[65]</sup>. The chemical

structures and properties of typical dyes and antibiotics are presented in Table 3. Indeed, dyes and antibiotics in the environment seriously threaten human health and ecological systems through bioaccumulation and disruption of biological processes. Therefore, it is crucial to implement strategies to reduce the wastewater concentration of these substances prior to discharge.

Industrial applications of dyes in sectors such as textiles, dyeing, paints, pharmaceuticals, and papermaking have expanded with industrialisation and improvements in living standards. However, this increased use has led to the generation of dye-containing wastewater. However, the structural diversity and complexity of dyes hinder their effective removal by some wastewater treatments, including coagulation, sedimentation, and biological treatment<sup>[71]</sup>. The presence of dyes can disrupt aquatic ecosystems by blocking sunlight, which inhibits photosynthetic organisms such as algae and aquatic plants, thereby reducing dissolved oxygen levels in the water<sup>[72]</sup>. Moreover, dyes possess diverse toxic properties that pose significant risks to human health and the environment, such as neurological disorders, organ toxicity, DNA damage, and adverse effects on aquatic organisms<sup>[73,74]</sup>.

Antibiotics are antimicrobial agents that inactivate bacteria or inhibit their growth and reproduction. However, the extensive and indiscriminate use of antibiotics in various sectors, including human medicine, veterinary practices, agriculture, livestock, poultry, and aquaculture, has led to significant release of these drugs into the environment. Additionally, the chemical stability and resistance to complete metabolism of pharmaceuticals often result in their incomplete removal from wastewater<sup>[75]</sup>. Antibiotic contamination is predominantly observed in water sources, including surface water, groundwater, sediments, soil, and drinking water<sup>[76]</sup>. Antibiotics

**Table 3** Chemical structures and properties of dyes (methylene blue, methyl orange, and malachite green) and antibiotics (tetracycline, ciprofloxacin, and levofloxacin)

Class	Chemical	Molecular formula	Structure	Molecular weight (g mol <sup>-1</sup> )	$\lambda_{\max}$ (nm)	Ref.
Dye	Methylene blue	C <sub>16</sub> H <sub>18</sub> ClN <sub>3</sub> S		319.85	672	[66]
	Methyl orange	C <sub>14</sub> H <sub>14</sub> N <sub>3</sub> NaO <sub>3</sub> S		327.33	467	[66]
	Malachite green	C <sub>52</sub> H <sub>56</sub> N <sub>4</sub> O <sub>12</sub>		364.91	614	[67]
Antibiotics	Tetracycline	C <sub>22</sub> H <sub>24</sub> N <sub>2</sub> O <sub>8</sub>		444.435	359	[68]
	Levofloxacin	C <sub>18</sub> H <sub>20</sub> FN <sub>3</sub> O <sub>4</sub>		361.368	289	[69]
	Ciprofloxacin	C <sub>17</sub> H <sub>18</sub> FN <sub>3</sub> O <sub>3</sub>		331.346	277	[70]

pose considerable risks to living organisms and environmental health. In living organisms, they can cause organ toxicity, allergic reactions, and gut microbiota disruption<sup>[77,78]</sup>. Environmentally, antibiotics are toxic to aquatic organisms, inhibit algal growth, and disrupt the ecological balance by affecting nontarget species<sup>[77,79]</sup>. In addition, their presence in water fosters genetic mutations and promotes the emergence of antibiotic-resistant pathogenic bacteria<sup>[80]</sup>. The major sources and the health and environmental impacts of the representative dyes (methylene blue [MB], methyl orange [MO], and malachite green [MG]) and antibiotics (tetracycline [TC], ciprofloxacin [CIP], and levofloxacin [LEV]) are summarised in Table 4.

### Inorganic pollutants

Inorganic pollutants, particularly heavy metals, have become increasingly prevalent in the surrounding environment, primarily because of anthropogenic activities such as mining, industrial discharges, and agricultural practices. Heavy metals are highly soluble in aquatic environments and exist primarily as cations and oxyanions<sup>[60]</sup>. However, heavy metals are not biodegradable, which results in their persistence in the environment. The accumulation of heavy metals in the soil, groundwater, and surface water poses a serious risk to ecosystems. Moreover, their nonbiodegradability allows them to bioaccumulate throughout the food chain, leading to toxic effects on living organisms<sup>[85]</sup>. Exposure to heavy metals such as Pb, Cu, and Cd can result in substantial physiological damage, including liver toxicity, neurological disorders, and dermatological conditions<sup>[86]</sup>. Additionally,

given the complex and unpredictable behaviour of aquatic environments, effective strategies for removing heavy metals from these ecosystems remain limited. The major sources and adverse effects of representative heavy metals (Pb, Cu, and Cd) on human health and the environment are summarised in Table 5.

### Mobility of heavy metals in aqueous solutions

The pH of an aqueous solution influences the distribution of heavy metal species and the efficiency of their adsorption onto biochar. At a low pH, heavy metals tend to exist predominantly as free ions, which are more soluble and mobile. These positively charged heavy metal ions are easily attracted to negatively charged biochar surfaces through electrostatic interactions, enhancing their adsorption capacity. As the pH increases, heavy metals may form hydroxide complexes that are less soluble and mobile. Within this pH range, biochar can effectively remove heavy metals through surface precipitation or complexation, thereby enhancing their immobilisation. Therefore, optimising the pH of an aqueous solution is crucial for maximising the adsorption capacity for heavy metal removal<sup>[92]</sup>. Furthermore, understanding the speciation changes in heavy metals as a function of pH is important. Pb predominantly exists as  $Pb^{2+}$  at pH < 6,  $Pb(OH)^+$  at pH 6–9,  $Pb(OH)_2$  at pH 9–12, and  $Pb(OH)_3^-$  at pH > 12<sup>[93]</sup>. The prevalent species of Cu at pH < 6 are  $Cu^{2+}$  and  $Cu(OH)^+$  whereas at pH > 6, it is  $Cu(OH)_2$ <sup>[94]</sup>. The dominant Cd species at pH < 8 is  $Cd^{2+}$  and those in the range of 8–11 are  $Cd^{2+}$ ,  $Cd(OH)^+$ ,  $Cd(OH)_{2(aq)}$ , and  $Cd(OH)_3^-$ <sup>[95]</sup>. The primary Zn species are  $Zn^{2+}$  and  $Zn(OH)^+$  at pH < 10 and  $Zn(OH)_{2(aq)}$ ,  $Zn(OH)_3^-$ , and  $Zn(OH)_4^{2-}$  at pH > 10<sup>[96]</sup>.

**Table 4** The major pollution sources and adverse effects of representative dyes (methylene blue, methyl orange, and malachite green) and antibiotics (tetracycline, ciprofloxacin, and levofloxacin) on human health and the environment

Class	Chemical	Source of pollutants	Human health	Environmental hazard	Ref.
Dye	Methylene blue	Industrial: textile, paint, paper, cosmetics, plastic, leather manufacturing, food processing, and the pharmaceutical industry	Cyanosis, Heinz body, eye irritation, tachycardia, delirium, jaundice, tissue necrosis, gastrointestinal disturbances (nausea, vomiting, gastritis, and diarrhoea)	Growth inhibition (microalgae), pigment formation (microalgae), aquatic ecosystem imbalance	[81]
	Methyl orange	Industrial: textile, paint, paper, leather manufacturing, food processing, printing, and the pharmaceutical industry	Teratogenesis, mutagenesis, carcinogenesis, eye irritation, hypersensitivity, allergies, dermatitis, tachycardia, cyanosis, jaundice, quadriplegia, tissue necrosis, gastrointestinal disturbances (vomiting and diarrhoea)	Growth inhibition (bacterial), water colouration, sunlight penetration reduction, photosynthesis disturbance, reduction in dissolved oxygen and gas solubility, eutrophication	[72,82]
	Malachite green	Industrial: textile, paper, cosmetics, plastic, leather manufacturing, food processing, and the pharmaceutical industry Aquacultural: fungicide and antiseptics for aquaculture	Teratogenesis, mutagenesis, carcinogenesis, respiratory issues, chromosomal aberrations	Growth inhibition (bacterial, plant, and animal), genotoxicity, cytotoxicity, reproduction disturbance, mitochondrial dysfunction	[83]
Antibiotics	Tetracycline	Hospital wastewater treatment plants Industrial: pharmaceutical manufacturing Agricultural: livestock excreta, agricultural fertiliser, and aquaculture	Disturbs intestinal microflora, allergies, kidney and liver dysfunction, chromosomal aberrations, reproductive issues, tooth discolouration, gastrointestinal disturbances, intracranial hypertension, skin infections (rosacea), inhibition of protein synthesis	Genetic mutation, emergence of antibiotic-resistant bacteria, impact on nontarget organisms, aquatic ecosystem imbalance	[76–78]
	Ciprofloxacin	Hospital wastewater treatment plants Industrial: pharmaceutical manufacturing Agricultural: livestock excreta, agricultural fertiliser	Genotoxicity, gastrointestinal disturbances (bleeding), leukopenia, neurological disorders, allergies	Genotoxicity, cytotoxicity, oxidative stress induction, emergence of antibiotic-resistant bacteria, growth inhibition (plant), toxicity to cyanobacteria	[79,84]
	Levofloxacin	Wastewater treatment plants Industrial: pharmaceutical manufacturing	Hormonal imbalance, reproductive toxicity, respiratory issues, carcinogenesis	Growth inhibition (algal), phytotoxicity, embryotoxicity, enhancement of plasmid transformability, toxicity to aquatic organisms (bacterial, plant, and animal)	[75]

**Table 5** The major pollution sources and adverse effects of representative heavy metals

Metal	Source of pollutants	Human health	Environmental hazard	Ref.
Pb	Industrial: steel, battery, pigment, paint, paper manufacturing, mining, smelting, electroplating, and petroleum refining Agricultural: pesticides and fertilisers	Gastrointestinal disturbances, kidney and liver dysfunction, neurological disorders (anaemia), reproductive toxicity, cognitive impairment	–	[87]
Cu	Industrial: steel, brass, pigments, paint, explosives manufacturing, mining, smelting, metallurgy, metal finishing, electroplating, and petroleum refining Agricultural: pesticides and fertilisers	Gastrointestinal disturbances (nausea, vomiting, and bleeding), kidney and liver dysfunction, neurotoxicity, reproductive issues (Wilson's disease), headache	Inhibition of microbial activity, affects earthworms, slows decomposition of organic matter	[88,89]
Cd	Industrial: electronics, electrode, battery, paint, ceramics manufacturing, mining, metallurgy, electroplating, and welding	Gastrointestinal disturbances, kidney and liver dysfunction, neurotoxicity, reproductive issues (anosmia), reproductive issues (urolithiasis), bone fragility, and carcinogenesis	Growth inhibition (plant), metabolism inhibition, photosynthesis disturbance, reduction of agricultural productivity	[90,91]

## Application of biochar to remove organic contaminants from wastewater

Organic pollutants are the most pervasive and detrimental contaminants affecting water quality worldwide. These pollutants, originating from diverse sources, such as industrial waste, agricultural runoff, and household waste, pose considerable challenges to environmental safety and public health<sup>[97]</sup>. In particular, nonbiodegradable dyes and antibiotics cause significant environmental challenges, including toxicity to aquatic organisms, inhibition of algal growth, and disruption of the ecological balance<sup>[74,77,79]</sup>. They are bio-refractory organic substances that can be harmful to aquatic organisms and human health. Therefore, the management and control of water contamination by organic dyes and antibiotics are critical. Among the existing wastewater treatment methods, adsorption has attracted attention for its ability to remove organic pollutants from wastewater.

## Mechanisms of organic contaminant adsorption

The adsorption of organic contaminants by manure biochar is driven by physical and chemical mechanisms. The porous properties of biochar, including its surface area, pore volume, and pore diameter, enable physical adsorption through hydrophobic interactions, van der Waals interactions, and pore filling. Chemically, O-containing functional groups (e.g.,  $-\text{COOH}$ ,  $-\text{OH}$ ,  $=\text{O}$ ) on the biochar's surface form hydrogen bonds and electrostatic interactions, whereas aromatic C domains mediate  $\pi$ - $\pi$  electron donor-acceptor interactions<sup>[98]</sup>. Additionally, the mineral components inherent in manure biochar (e.g.,  $\text{Ca}^{2+}$  and  $\text{Mg}^{2+}$ ) facilitate surface precipitation through complexation with ionic pollutants or chelation of organic compounds. The combined effects of these mechanisms allow manure-derived biochar to immobilise diverse organic pollutants effectively. Fig. 3 shows the different adsorption mechanisms of organic contaminants on biochar.

### Physical adsorption mechanisms

#### Hydrophobic interactions and van der Waals forces

The hydrophobic interactions in biochar are primarily attributed to the attraction between its nonpolar surface and hydrophobic organic contaminants<sup>[99]</sup>. The nonpolar surface of biochar results from C-rich and aromatic C structures within the biochar matrix. Therefore, biochar's hydrophobicity significantly influences its adsorption capacity for hydrophobic and neutral organic contaminants in wastewater. Van der Waals forces in biochar-based adsorption involve weak, transient dipole-induced interactions between the nonpolar C-rich surfaces of biochar and the hydrophobic contaminants<sup>[100]</sup>. These interactions are facilitated by fluctuations in the electron distribution, which generate instantaneous dipoles<sup>[101]</sup>. Hydrophobic interactions and van der Waals forces can be enhanced by developing aromatic C structures and increasing the biochar's surface area<sup>[102]</sup>. The desired

modifications can be accomplished by increasing the pyrolysis temperature, which facilitates carbonisation and graphitisation while increasing the accessibility of adsorption sites on the biochar's surface. Tsui & Roy<sup>[103]</sup> investigated the adsorption capacity of compost-derived biochar for atrazine, a hydrophobic organic compound, and observed that the adsorption capacity increased with the pyrolysis temperature across a range from 320 to 720 °C. This increase was attributed to the enhanced hydrophobicity resulting from the decrease in O content of the biochar. Hydrophobic interactions and van der Waals forces synergise with pore-filling mechanisms, whereby contaminants are physically located within the pores.

#### Pore-filling

Pore-filling is a key adsorption mechanism whereby contaminants are physically retained within the porous network of biochar because of their size compatibility. Since the pore-filling process depends on the pore size of the biochar, enhancing its porosity and surface area is crucial because it provides a more accessible adsorption area<sup>[104]</sup>. Porosity and surface area are particularly significant in biochars produced at high pyrolysis temperatures. In addition, because pore-filling in biochar is primarily governed by hydrophobic interactions and van der Waals forces, a nonpolar surface further enhances its adsorption capacity<sup>[105]</sup>. The surface's nonpolarity can

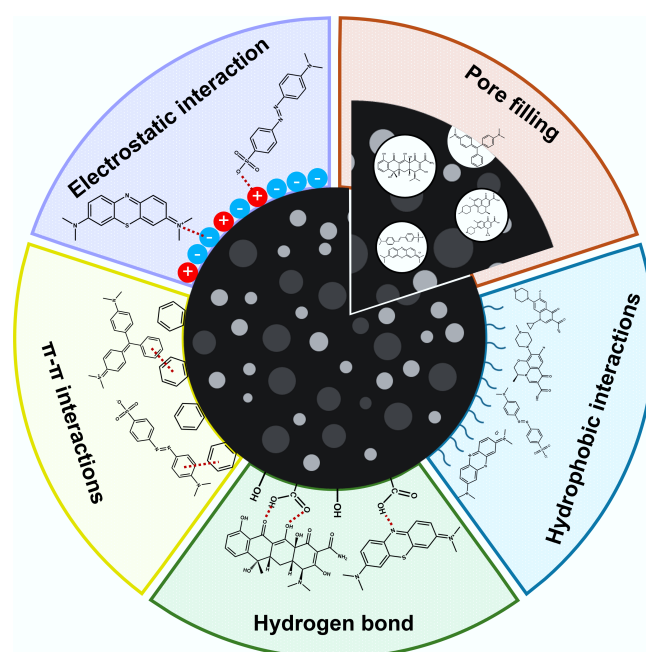


**Fig. 3** Mechanisms of the adsorption of organic pollutants by biochar.



be evaluated by assessing the atomic H/C ratio. Wei et al.<sup>[106]</sup> reported that when the H/C ratio decreased below 0.5, the contribution of pore-filling to the overall adsorption of herbicides increased significantly. This finding is supported by a study by Wang & Jang<sup>[107]</sup>, who investigated LEV adsorption using swine manure-derived biochar. Using a dual-mode adsorption model, their study demonstrated that pore-filling dominates in biochar produced at higher pyrolysis temperatures. The dual-mode model reflects preferential interactions between the solutes and the pore-filling domains within the biochar matrix<sup>[106]</sup>. Elevated pyrolysis temperatures improved the pore structure, as reflected by the higher specific surface area, pore volume, and mean pore diameter, and decreased the H/C ratio, collectively amplifying the role of pore-filling in the adsorption of recalcitrant organic pollutants. Although pore-filling dominates under these conditions, it is important to recognise that physical and chemical adsorption processes occur simultaneously. Therefore, a comprehensive investigation of the chemical adsorption mechanism of biochar is essential to fully understand its adsorption behaviour.

### Hydrogen bonds

Hydrogen bonds refer to the electrostatic attraction between a hydrogen atom bonded to an electronegative atom (such as N, O, or F), and another electronegative atom in other molecules. Hydrogen bonding is primarily driven by the partial positive charge of hydrogen, induced by electronegative atoms, which enables electrostatic attraction with the neighbouring electronegative atoms<sup>[108]</sup>. Biochar typically contains abundant O-containing functional groups such as hydroxyl (–OH), carboxyl (–COOH), carbonyl (–C=O), and amine (–NH) groups<sup>[109]</sup>. These functional groups can act as hydrogen bond donors and acceptors, facilitating strong and selective interactions with pollutants bearing complementary functional moieties<sup>[110]</sup>. Consequently, organic compounds that contain complementary functional groups, including dyes, pharmaceuticals, and pesticides, can be effectively adsorbed onto biochar via hydrogen-bonding interactions. Zhuo et al.<sup>[111]</sup> demonstrated that the adsorption mechanism of TC on Ca-modified corn stover biochar was caused by hydrogen bonding between the O-containing functional groups (C–O and O–C=O) on the biochar and the complementary functional groups of TC molecules.

### Chemical adsorption mechanisms

#### Electrostatic interactions

Electrostatic interactions in biochar adsorption refer to the attraction between the charged sites on the biochar's surface and oppositely charged pollutant molecules. Biochar's surfaces typically exhibit a net negative charge, primarily owing to the presence of O-containing functional groups such as carboxyl and hydroxyl groups. This negative surface potential promotes the adsorption of positively charged species, including metal ions and certain cationic pollutants. The strength and selectivity of the electrostatic interactions are governed by factors such as the ash content and the abundance and type of surface functional groups<sup>[112]</sup>. In addition, the solution's pH has a significant influence on the electrostatic interactions by modifying the surface charge of the biochar. A key concept in this context is the point of zero charge ( $pH_{pzc}$ ), at which the biochar surface exhibits a net neutral charge owing to an equal balance of positive and negative surface charges<sup>[113]</sup>. When the solution's pH is below the  $pH_{pzc}$ , the biochar surface acquires a net positive charge, favouring the adsorption of negatively charged species (anions). In contrast, when the pH exceeds the  $pH_{pzc}$ , the surface adopts a negative charge, facilitating the adsorption of positively charged species (cations). This transition in the surface charge with increasing pH can be attributed to the deprotonation of functional groups, which leads to a more

negatively charged surface<sup>[114]</sup>. In addition to the charge characteristics of biochar, the ionic nature of the target pollutants significantly influences the electrostatic interactions<sup>[115]</sup>. For example, the efficiency of removing MB, a cationic dye, improves with an increase in pH (from 2 to 10) because the negatively charged surface of biochar at an elevated pH enhances the electrostatic attraction<sup>[116]</sup>. The adsorption capacity of biochar for TC tends to decrease with an increase in pH, as TC becomes negatively charged at higher pH levels ( $TC^+$  at  $pH < 3.3$ ,  $TC^0$  at  $pH 3.3–7.7$ ,  $TC^-$  at  $pH 7.7–9.7$ , and  $TC^{2-}$  at  $pH > 9.7$ )<sup>[117]</sup>. This results in electrostatic repulsion between the negatively charged TC and similarly charged surfaces of the biochar<sup>[118]</sup>. Figure 4 shows the distribution of recalcitrant organic pollutant species as a function of the pH value<sup>[119–121]</sup>.

#### The $\pi$ – $\pi$ EDA interaction

The  $\pi$ – $\pi$  EDA interaction or  $\pi$ – $\pi$  stacking is primarily driven by electrostatic attraction arising from differences in electron density between  $\pi$ -systems. In these interactions, an electron-rich  $\pi$ -system (donor) engages with an electron-deficient  $\pi$ -system (acceptor) via orbital overlap and charge transfer, resulting in attractive forces. The electron-rich  $\pi$ -system typically stems from the incorporation of electron-donating groups (e.g., hydroxyl and amine groups) into a conjugated structure (e.g., aromatic rings), whereas the electron-deficient  $\pi$ -system is formed by the presence of electron-withdrawing groups (e.g., carboxylic acid, nitro, and ketone groups)<sup>[100]</sup>. Biochar typically possesses O-containing functional groups, including hydroxyl (–OH) and carbonyl (–C=O) groups, attached to aromatic rings, which can serve as electron acceptors and facilitate  $\pi$ – $\pi$  EDA interactions<sup>[123]</sup>. These interactions are particularly pronounced with organic pollutants that exhibit complementary  $\pi$ -systems, such as pharmaceuticals and dyes (Table 3)<sup>[124]</sup>. Accordingly, to enhance the adsorption capacity of biochar for organic pollutants via  $\pi$ – $\pi$  EDA interactions, implementing activation treatments is crucial. These treatments introduce or modify the surface functional groups that impart suitable electron-donating or electron-accepting characteristics, depending on the target contaminants.

### Adsorption of dyes

Dyes are used extensively in various industries, resulting in the discharge of wastewater containing residual dyes. Because of their complex molecular structures, dyes are resistant to conventional treatments such as coagulation, sedimentation, and biological processes. Their persistence in aquatic environments disrupts photosynthesis, reduces O levels, and poses toxic risks to ecosystems and public health<sup>[125]</sup>. Consequently, adsorption has gained increasing attention as an effective method for removing recalcitrant organic pollutants from wastewater. Table 6 presents dye adsorption from wastewater by animal manure biochar. The adsorption of dyes by biochar is largely attributed to the functional groups present on its surface, which facilitate various interactions with the dye molecules<sup>[109]</sup>.

The viability of animal manure biochar as an adsorbent for dye removal was demonstrated in a comparative study by Ahmad et al.<sup>[126]</sup>. This investigation focused on removing MB from an aqueous solution using biochar produced from bovine manure, rice husks, and sludge. Compared with that of rice husk and sludge biochar, bovine manure biochar demonstrated consistently high MB removal efficiency, maintaining a removal rate of 97.0%–99.0% across a pH range of 2.0–11.0. This high efficiency is likely attributable to the abundance of carboxyl (–COO) groups and the larger pore size on the surface of bovine manure biochar, providing active sites for adsorption.

The properties of manure vary depending on the animal species, which, in turn, influence the surface properties of the resulting



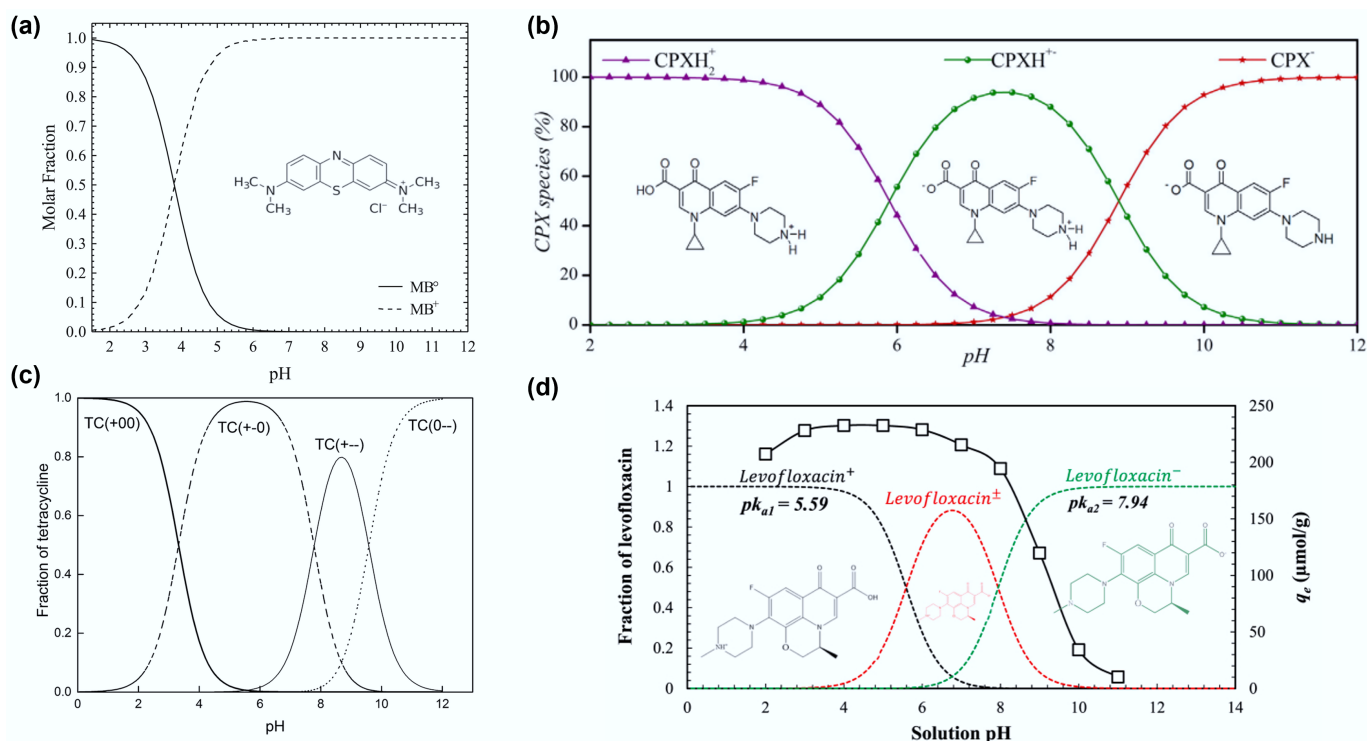


**Fig. 4** Distribution of (a) methylene blue (reprinted from Salazar-Rabago et al.<sup>[119]</sup> with the permission of Elsevier), (b) ciprofloxacin (reprinted from Roca Jalil et al.<sup>[122]</sup> with the permission of Elsevier), (c) tetracycline (reprinted from Wang et al.<sup>[120]</sup> with permission; copyright 2018 Royal Society of Chemistry), and (d) levofloxacin (reprinted from Shaha et al.<sup>[121]</sup> with the permission of Elsevier) at different pH values.

**Table 6** Application of animal manure biochar for dye adsorption

Target	Adsorbent	Pyrolysis and activation conditions	Surface area (m <sup>2</sup> g <sup>-1</sup> )	Total pore volume (cm <sup>3</sup> g <sup>-1</sup> )	Average pore diameter (nm)	Ash content (wt.%)	H/C ratio	O/C ratio	Qmax (mg g <sup>-1</sup> )	Ref.
Methylene blue	Bovine	Biochar: 500 °C for 3 h							17.50	[126]
Methylene blue	Sheep	Biochar: 500 °C for 2 h	160.53	0.172	10.03	17.82	0.037	0.244	202.72	[127]
Methylene blue	Rabbit	Biochar: 500 °C for 2 h	21.14	0.041	8.64	15.38	0.064	0.165	86.85	[127]
Methylene blue	Swine	Biochar: 500 °C for 2 h	13.36	0.025	7.33	13.14	0.128	0.079	46.95	[127]
Methylene blue	Bovine	Biochar: 200 °C	0.3276	0.00613	75.02				192.31	[133]
Methyl orange	Chicken	Biochar: 600 °C for 2 h							39.47	[128]
Methyl orange	Sheep	Biochar: 600 °C for 2.5 h	181.76	0.245			0.035	0.191	42.51	[129]
Malachite green	Sheep	Biochar: 450 °C	11.731						208.33	[130]
Methylene blue	Swine	Biochar: 700 °C for 2 h; Activation: alkali fusion pretreatment of fly ash	209.1	0.369	7.10			0.43	142.86	[135]

biochar. Therefore, comparative analyses of the adsorption capacity of biochar derived from the manure of various animals are required. Huang et al.<sup>[127]</sup> evaluated the adsorption performance of three manure biochars (sheep, rabbit, and swine manure) for the removal of MB from aqueous solutions. The surface area, pore volume, and pore size of sheep manure biochar (160.53 m<sup>2</sup> g<sup>-1</sup>, 0.172 cm<sup>3</sup> g<sup>-1</sup>, and 10.03 nm, respectively) were larger than those of rabbit (21.14 m<sup>2</sup> g<sup>-1</sup>, 0.041 cm<sup>3</sup> g<sup>-1</sup>, and 8.64 nm, respectively) and swine manure biochar (13.36 m<sup>2</sup> g<sup>-1</sup>, 0.025 cm<sup>3</sup> g<sup>-1</sup>, and 7.33 nm, respectively). Furthermore, sheep manure biochar demonstrated a higher O/C ratio and a lower H/C ratio than rabbit and swine manure biochars. These characteristics indicate that sheep manure biochar offers more adsorption sites for MB, and its greater polarity and aromaticity enhance physical and chemical adsorption mechanisms, including pore-filling, electrostatic interaction, hydrogen bonding, and  $\pi$ - $\pi$  EDA interactions. Sheep manure biochar exhibited a higher adsorption capacity for MB (202.729 mg g<sup>-1</sup>) than rabbit (86.852 mg g<sup>-1</sup>) or swine manure biochar (46.958 mg g<sup>-1</sup>).

In recent years, studies on the adsorption-based treatment of MO in wastewater have increased. Nevertheless, research investigating the use of manure biochar as an adsorbent for MO remains limited. Yu et al.<sup>[128]</sup> investigated the adsorption of MO using chicken manure biochar, pyrolyzed at 600 °C for 120 min, and reported a maximum adsorption capacity of 39.47 mg g<sup>-1</sup>. Similarly, Lu et al.<sup>[129]</sup> evaluated sheep manure biochar produced at 600 °C for 150 min, which demonstrated a higher MO adsorption capacity of 42.51 mg g<sup>-1</sup>. These results indicate that the adsorption capacity of MO using sheep manure biochar was more significant than that of chicken manure biochar. This is consistent with MB removal, and sheep manure biochar showed greater adsorption performance than other animal manure biochars. This enhanced performance may be attributed to the higher plant fibre content in sheep manure, which likely contributes to the greater specific surface area and higher content of O-containing functional groups in the resulting biochar (Fig. 5).

The detailed adsorption mechanisms of using sheep manure biochar as an adsorbent were studied by Dilekoğlu<sup>[130]</sup> with MG. The

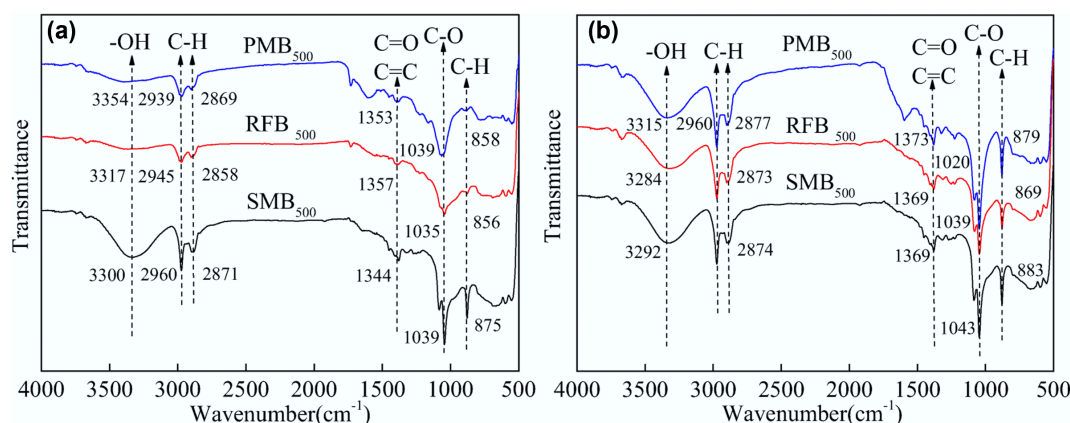


**Fig. 5** FT-IR spectra of pig (blue), rabbit (red), and sheep (black) manure biochar (a) before and (b) after adsorption of methylene blue. Reprinted from Huang et al.<sup>[127]</sup> with the permission of Springer Nature.

biochar was produced at 450 °C, and the maximum adsorption capacity was 208.33 mg g<sup>-1</sup>. To investigate the adsorption mechanism of MG, changes on the biochar surface were observed using Fourier transform infrared (FT-IR) spectroscopy. After the adsorption of MG, the FT-IR spectra of the biochar showed shifts in the -OH and C-H peak regions. This indicated the involvement of multiple interactions, including electrostatic attraction between MG and the -OH groups, hydrogen bonding between the N-heterocyclic ring of MG and the -OH groups, and  $\pi$ - $\pi$  EDA interactions between the aromatic rings of MG and the C-H groups<sup>[131]</sup>. These findings are consistent with the thermodynamic parameters of MG adsorption, with a calculated change in enthalpy of 56,674 kJ mol<sup>-1</sup>. Notably, the value of > 60 kJ mol<sup>-1</sup> suggests that chemical adsorption is the predominant mechanism governing this process<sup>[132]</sup>.

Adsorption parameters such as the solution's pH and biochar's surface properties were investigated to optimise the performance of biochar for organic pollutant removal. Notably, the solution's pH affects the ionisation state of the biochar's surface and the pollutants, thereby altering the electrostatic interactions and adsorption capacity. Dilekoğlu<sup>[130]</sup>, using sheep manure biochar, demonstrated that the capacity to adsorb MG, a cationic dye, reached equilibrium at high pH values ( $\geq 4$  pH). This was attributed to competition between the MG and excess hydrogen ions for adsorption sites under acidic conditions. When the solution's pH exceeded the  $pH_{pzc}$  of the biochar, the surface became negatively charged, which enhanced the electrostatic attraction between the biochar and MG. In contrast, Yu et al.<sup>[128]</sup> reported that chicken manure biochar exhibited a higher adsorption capacity for MO, an anionic dye, under acidic conditions. Notably, at an elevated pH, competition from hydroxide ions (OH<sup>-</sup>) reduces the adsorption of MO. Furthermore, under acidic conditions, protonation of the surface functional groups (e.g., -OH<sub>2</sub><sup>+</sup> and -NH<sub>3</sub><sup>+</sup>) promotes the electrostatic attraction of anionic MO. Optimising the solution's pH according to the ionic nature of the target dye is critical for maximising the adsorption performance.

Surface properties, such as surface area, porosity, and the abundance of functional groups, are key factors governing the availability of adsorption sites on biochar and, consequently, their overall adsorption capacity. The pyrolysis temperature significantly influences these properties, thereby affecting the adsorption capacity. Zhu et al.<sup>[133]</sup> investigated the effect of the pyrolysis temperature on the adsorption capacity of bovine manure biochar for MB. As the temperature increased from 200 to 800 °C, the surface area and pore volume of the biochar increased from 0.3276 m<sup>2</sup> g<sup>-1</sup> and

0.00613 cm<sup>3</sup> g<sup>-1</sup> to 3.627 m<sup>2</sup> g<sup>-1</sup> and 0.0107 cm<sup>3</sup> g<sup>-1</sup>, respectively. However, the pore size decreased from 75.02 to 12.979 nm. Interestingly, despite exhibiting a greater specific surface area and higher porosity, bovine manure biochar produced at 800 °C showed lower adsorption performance than that produced at 200 °C. This could be attributed to the substantial loss of O-containing functional groups, including carboxyl, lactonic, and phenolic groups, at elevated pyrolysis temperatures. These functional groups are critical for facilitating various adsorption mechanisms such as electrostatic interactions, hydrogen bonding, and cation exchange.

In addition to modifying the operational parameters, the activation of biochar to enhance its adsorption capacity for dye removal was also investigated. This is commonly achieved through impregnation with iron oxide, manganese oxide, or alkaline earth metals<sup>[134]</sup>. This treatment improved the specific surface area, porosity, and the number of O-containing functional groups on the biochar's surface. Wang et al.<sup>[135]</sup> modified swine manure biochar using alkali-fused fly ash (AFFA) to increase its capacity for MB adsorption. This modification improved the surface area and porosity of the swine manure biochar. Furthermore, it preserved O-containing functional groups, such as -OH and C=O, at a pyrolysis temperature of 700 °C. The abundant O-containing functional groups, along with the aromatic structure of AFFA-activated biochar facilitate multiple adsorption mechanisms, including  $\pi$ - $\pi$  EDA interactions, electrostatic interactions, and hydrogen bonding. Notably, the aromatic structure increases with increasing pyrolysis temperature. Additionally, the notable concentration of Na<sup>+</sup> in the activated swine manure biochar potentially contributed to its ion exchange capacity. Consequently, AFFA-activated swine manure biochar exhibited a 10.7%–112.3% increase in MB adsorption capacity.

Dye removal by animal manure biochars is driven by electrostatic interactions,  $\pi$ - $\pi$  EDA interactions, and hydrogen bonding, with the relative contribution of each mechanism determined by both the ionic nature of the dye and the surface chemistry of the biochar. In unmodified biochars, electrostatic attraction occurs between oppositely charged dye molecules and the biochar's surface,  $\pi$ - $\pi$  EDA interactions arise from the association between aromatic dye structures and graphitic domains in the biochar, and hydrogen bonding is facilitated by O-containing functional groups such as -OH and -COOH. Among various feedstocks, sheep manure biochar consistently achieves higher adsorption capacities for MB, MO, and MG because of its greater specific surface area and higher O/C ratio compared with other animal manures. The pH-dependent behaviour reflects the charge characteristics of the dye, with

cationic dyes such as MB and MG exhibiting maximum adsorption when the surface is negatively charged ( $\text{pH} > \text{pH}_{\text{pzc}}$ ). In contrast, anionic dyes such as MO show higher adsorption under acidic conditions through protonation of the surface's functional groups. Given the inherently high ash content of manure, which imparts alkalinity, manure-derived biochar tends to be more suitable for cationic dye adsorption. In alkali-metal-modified biochars, enhanced dye removal performance is achieved through increased surface area, porosity, and O-containing functional groups, which intensify hydrogen bonding and  $\pi$ - $\pi$  EDA interactions, while alkaline metals introduced during activation can contribute to additional ion exchange mechanisms.

## Adsorption of antibiotics

Antibiotics are antimicrobial agents used across the human, veterinary, and agricultural sectors, which has led to their widespread release into the environment. Their chemical stability and incomplete metabolism hinder their removal during conventional wastewater treatment, resulting in contamination of surface water, groundwater, soil, and sediment. These compounds pose significant risks to living organisms by causing organ toxicity, allergic reactions, and disruption of gut microbiota. In the environment, antibiotics harm aquatic organisms, suppress algal growth, and disturb the ecological balance by affecting nontarget species<sup>[136]</sup>. Moreover, their persistence in water promotes genetic mutations and accelerates the development of antibiotic-resistant bacteria<sup>[137]</sup>. Therefore, the development of effective treatment strategies, such as biochar-based adsorption, is essential for mitigating antibiotic contamination in aquatic environments. Antibiotics adsorption from aquatic environments using animal manure biochar is presented in Table 7.

Understanding the adsorption mechanism is essential for optimising the adsorption capacity of antibiotics. Wang et al.<sup>[120]</sup> investigated TC adsorption on swine manure biochar and compared it with that on rice straw biochar. The adsorption data fitted both the Freundlich and Langmuir models well, suggesting the involvement of both physical and chemical mechanisms<sup>[138]</sup>. In particular, a strong correlation between the specific surface area and Langmuir adsorption capacity was observed. However, the poor fit of the Temkin model and the weak correlation with O-containing functional groups suggest that electrostatic interactions and hydrogen bonding were not dominant<sup>[109]</sup>. Higher adsorption capacities were observed at pH 3.5–8.0, where TC exists as a zwitterion and interacts with the negatively charged biochar surface via  $\pi$ - $\pi$  EDA interactions. The conjugated enone structure of TC acts as a  $\pi$ -electron acceptor, whereas the graphite-like biochar serves as a  $\pi$ -electron donor<sup>[139]</sup>. These findings suggest that  $\pi$ - $\pi$  EDA interactions are crucial in the adsorption of TC onto swine manure biochar. These results are consistent with those of Zhao et al.<sup>[117]</sup>, who investigated the TC adsorption mechanisms of bovine manure biochar at pyrolysis temperatures ranging from 500 to 700 °C. An increase in

the pyrolysis temperature improved the maximum adsorption capacity of the bovine manure biochar. However, this was accompanied by a reduction in the number of surface functional groups, including acidic, phenolic hydroxyl, carbonyl, and lactone groups. This suggests that the primary mechanisms responsible for the adsorption of TC by bovine manure biochar were hydrophobic interactions and  $\pi$ - $\pi$  EDA interactions. Nevertheless, given that TC contains multiple O-containing functional groups, the overall adsorption capacity remained low, suggesting that activation strategies aimed at enriching the surface functional groups of manure-derived biochar are essential.

Similarly, Wang & Jang<sup>[107]</sup> conducted an investigation on LEV's adsorption mechanism using swine manure biochar produced at pyrolysis temperatures ranging from 300 to 900 °C. The highest adsorption capacity (158 mg g<sup>-1</sup>) was achieved with swine manure biochar produced at 900 °C. To evaluate the adsorption behaviour and maximum capacity, five isotherm models, namely, the Langmuir, Freundlich, Temkin, Dubinin–Radushkevich, and dual-mode models, were employed. The results indicated that LEV's adsorption onto high-temperature swine manure biochar followed a multilayer adsorption pattern involving chemical mechanisms, such as electrostatic interactions, hydrogen bonding, cation- $\pi$ , and  $\pi$ - $\pi$  EDA interactions, and physical mechanisms, including pore-filling (Fig. 6).

Additionally, Huang et al.<sup>[140]</sup> investigated the removal mechanism of CIP using rabbit manure biochar (RMB) produced at pyrolysis temperatures ranging from 400 to 700 °C. RMB produced at 700 °C exhibited the highest adsorption capacity (70.17 mg g<sup>-1</sup>) for CIP. Isothermal and thermodynamic analyses revealed that the adsorption behaviour was better described by the Langmuir model, indicating monolayer adsorption<sup>[138]</sup>. The enthalpy change ( $\Delta H = 31.88 \text{ kJ mol}^{-1}$ ) suggested that hydrogen bonding was the primary adsorption mechanism<sup>[141]</sup>, involving interactions between the N-containing heterocyclic ring, -COOH, and -F groups in CIP and the O-containing functional groups on RMB. Indeed, as the pyrolysis temperature increased, the degree of graphitisation and aromaticity in RMB also increased, enhancing  $\pi$ - $\pi$  EDA interactions. These  $\pi$ - $\pi$  interactions were facilitated by the electron-accepting groups in CIP (-COOH and -F) and the  $\pi$ -electron-donating sites in RMB (e.g., C-H in aromatic structures).

Animal manure biochar exhibits a limited surface area, pore structure, and functional group availability because of the inherent characteristics of the raw material, which constrain its maximum capacity to adsorb antibiotic compounds. Therefore, the modification of animal manure biochar has been investigated to enhance its capacity to adsorb antibiotics. Chen et al.<sup>[142]</sup> modified swine manure biochar using acid (14% H<sub>3</sub>PO<sub>4</sub>) for adsorbing TC. This modification increased the surface area from 227.56 to 319.04 m<sup>2</sup> g<sup>-1</sup>, and the pore volume from 0.14 to 0.25 cm<sup>3</sup> g<sup>-1</sup>. Additionally, H<sub>3</sub>PO<sub>4</sub> modification enhanced the O-containing functional groups (-COOH and -OH) on the biochar's surface<sup>[143]</sup>. After H<sub>3</sub>PO<sub>4</sub> modification, the

**Table 7** Applications of animal manure biochar for the adsorption of antibiotics

Target	Adsorbent	Pyrolysis and activation conditions	Surface area (m <sup>2</sup> g <sup>-1</sup> )	Total pore volume (cm <sup>3</sup> g <sup>-1</sup> )	Average pore diameter (nm)	Ash content (wt.%)	H/C ratio	O/C ratio	Q <sub>max</sub> (mg g <sup>-1</sup> )	Ref.
Tetracycline	Swine	Biochar: 600 °C for 2 h	10.56	0.044	12.36		0.05	0.250	8.125	[120]
Tetracycline	Bovine	Biochar: 700 °C							5.82	[117]
Tetracycline	Swine	Biochar: 700 °C for 2 h Activation: 14% H <sub>3</sub> PO <sub>4</sub> solution for 24 h at 25 °C	319.04	0.25		43.9	0.01	0.06	160.3	[142]
Levofloxacin	Swine	Biochar: 900 °C for 2 h	512.11	0.51	4.008	18.39 <sup>a</sup>	0.014	0.093	158.07	[107]
Ciprofloxacin	Rabbit	Biochar: 700 °C for 2.5 h	91.52	0.237	12.64	19.06	0.032	0.276	57.626	[140]

<sup>a</sup> After acid washing.

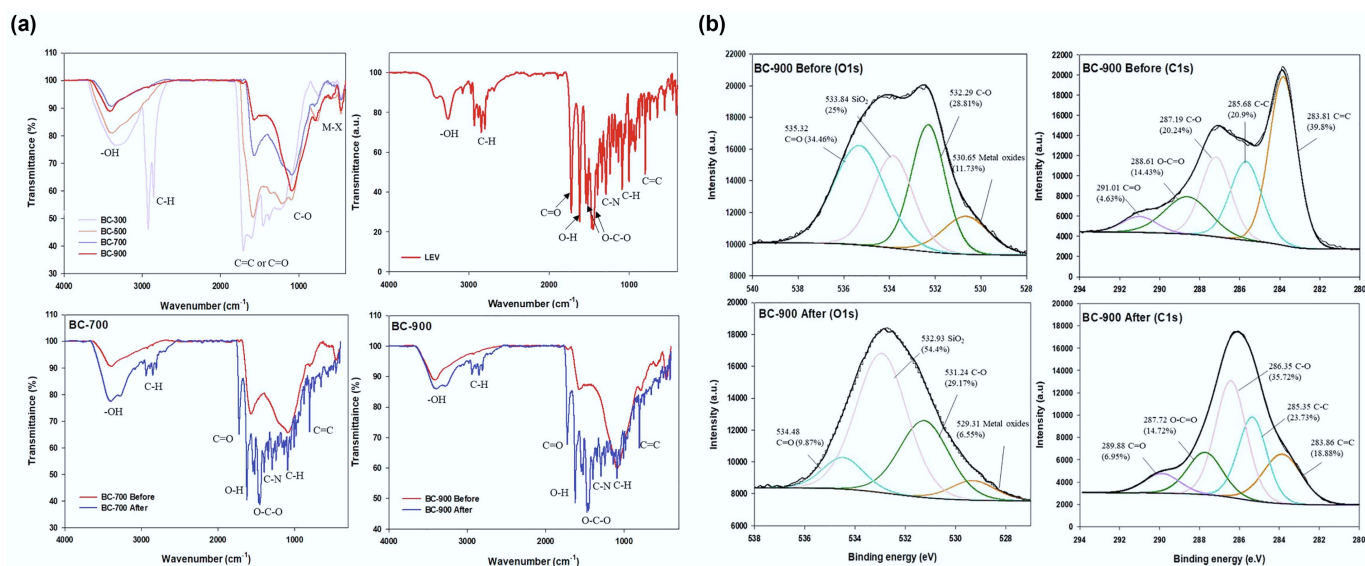


**Fig. 6** (a) FT-IR spectra and (b) X-ray photoelectron spectroscopy (XPS) spectra (O1s and C1s) of swine manure biochar before and after adsorption of levofloxacin. Reprinted from Wang & Jang<sup>[107]</sup> with the permission of Elsevier.

adsorption capacity of swine manure biochar increased. In conclusion, the enhanced TC adsorption was attributed primarily to chemisorption mechanisms, including hydrogen bonding and  $\pi$ - $\pi$  EDA interactions.

Animal manure biochar effectively adsorbs TC, with optimal performance observed at pH 3.5–8.0 where TC exists as a zwitterion. Adsorption occurs mainly via  $\pi$ - $\pi$  EDA interactions between the conjugated enone structure of TC and the aromatic domains of biochar. Higher pyrolysis temperatures enhance hydrophobicity, which strengthens  $\pi$ - $\pi$  EDA interactions and increases the adsorption capacity despite the loss of acidic and phenolic groups. Nevertheless, due to the presence of numerous O-containing functional groups in TC, adsorption using manure-derived biochar is negligible. As such, surface modification is necessary. Surface modification with  $\text{H}_3\text{PO}_4$  further improves TC adsorption by increasing the surface area, enhancing the O-containing functional groups, and promoting hydrogen bonding alongside  $\pi$ - $\pi$  EDA interactions. For LEV, swine manure biochar pyrolysed at 900 °C achieved the highest adsorption capacity, with removal governed by multilayer chemical and physical mechanisms including electrostatic attraction, hydrogen bonding, cation- $\pi$  interactions,  $\pi$ - $\pi$  EDA interactions, and pore filling. Rabbit manure biochar produced at 700 °C exhibited the highest adsorption capacity for CIP, characterised by monolayer adsorption dominated by hydrogen bonding between CIP functional groups (-COOH, -F, N-heterocycles) and O-containing sites on the biochar's surface, supplemented by  $\pi$ - $\pi$  EDA interactions enhanced by greater aromaticity at higher temperatures. The differing properties of each antibiotic result in distinct adsorption mechanisms. Therefore, biochar should be tailored to the specific characteristics of each antibiotic.

## Application of biochar to remove heavy metals from wastewater

Heavy metals are prevalent pollutants in wastewater, primarily originating from industrial activities such as battery production, electroplating, and mining. Their nonbiodegradable nature and high toxicity render them hazardous to humans, animals, and plants, even

at low concentrations. Consequently, various treatment technologies, including redox processes, chemical precipitation, and membrane separation, have been developed for their removal. Among these methods, adsorption has gained attention because of its technical simplicity and low cost<sup>[144]</sup>. Biochar is considered a promising adsorbent owing to its high porosity, high surface activity, and the abundance of functional groups. However, its adsorption capacity depends on factors such as the type of heavy metal and the pyrolysis conditions, highlighting the need for performance evaluation for targeted applications.

## Mechanisms of heavy metal adsorption

Adsorption of heavy metals by biochar involves a combination of various mechanisms, including physical adsorption, electrostatic interactions, precipitation, ion exchange, and surface complexation (Fig. 7)<sup>[144]</sup>. The predominant adsorption mechanisms can vary depending on the target metals and physicochemical properties of the biochar.

### Physical adsorption

#### Hydrophobic interactions and van der Waals forces

The physical adsorption mechanism of heavy metals onto biochar primarily involves nonspecific interactions, particularly van der Waals forces, existing between the surface of the biochar and the heavy metal ions<sup>[145]</sup>. Biochar typically possesses a porous structure with a large surface area that allows metal ions to diffuse into its pores. Generally, the efficiency of physical adsorption is strongly determined by the pore size distribution and surface area of the biochar<sup>[146]</sup>. Accordingly, increasing the porosity and surface area of the biochar may improve its capacity to adsorb heavy metal ions. However, physical adsorption is typically not the dominant mechanism for used heavy metal adsorption because of its relatively weak adsorption affinity compared with chemical adsorption. For instance, Xu et al.<sup>[147]</sup> reported that rice husk biochar, despite having a larger surface area ( $27.8 \text{ m}^2 \text{ g}^{-1}$ ) than dairy manure biochar ( $5.61 \text{ m}^2 \text{ g}^{-1}$ ), exhibited five times lower adsorption capacities for Pb(II), Cu(II), Cd(II), and Zn(II). This suggests that chemical interactions play a more influential role in heavy metal adsorption.



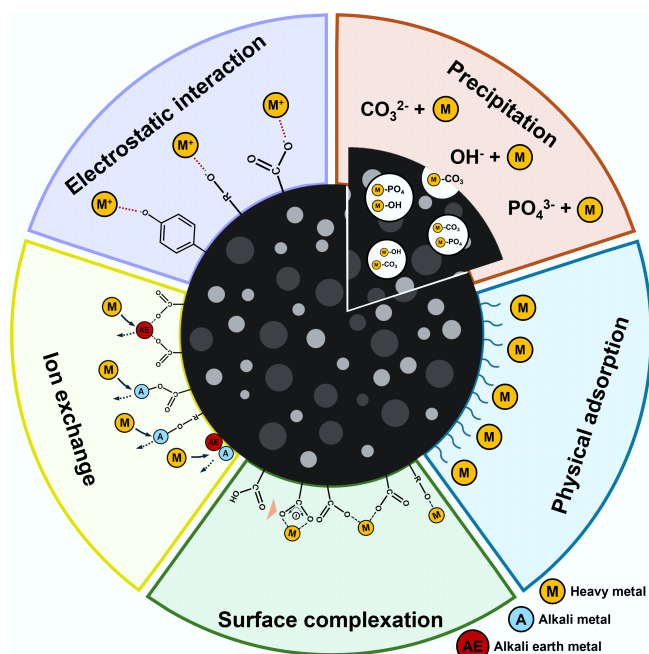


Fig. 7 Mechanisms for adsorption of heavy metals by biochar.

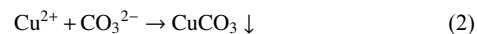
## Chemical adsorption

### Electrostatic interaction

Electrostatic interactions refer to attractive forces that occur between the surface charges on the biochar and heavy metal ions<sup>[148]</sup>. In particular, negatively charged biochar, resulting from the presence of O-containing functional groups, such as carboxylic (–COOH), hydroxyl (–OH), and phenol (Ar–OH) groups, can effectively attract heavy metal cations, including  $Pb^{2+}$ ,  $Cd^{2+}$ , and  $Cu^{2+}$ , in wastewater<sup>[149]</sup>. Considering that the charge on the biochar's surface and metal ions varies with solution pH, the effectiveness of the electrostatic interactions is highly dependent on the pH. For instance, when the solution's pH exceeds  $pH_{pzc}$ , the functional groups in biochar undergo deprotonation<sup>[150]</sup>. This results in the biochar imparting a negative charge, which facilitates its ability to attract positively charged metal ions via electrostatic interactions. Although electrostatic interactions contribute to adsorption, they are relatively weak compared with other mechanisms such as precipitation, ion exchange, and surface complexation, which play a more significant role in heavy metal adsorption. These processes involve stronger chemical interactions, leading to more stable and irreversible binding of metal ions. In this context, these mechanisms contribute significantly to the overall adsorption capacity and efficiency.

### Precipitation

The precipitation of heavy metals involves the formation and subsequent deposition of insoluble metal compounds within biochar's pores during the adsorption process. This process involves the reaction between metal ions and anions, including hydroxides ( $OH^-$ ), carbonates ( $CO_3^{2-}$ ), or phosphates ( $PO_4^{3-}$ ), released from the biochar, leading to the formation of precipitates<sup>[151]</sup>. The proposed precipitation reaction of  $Cu(II)$  is shown in Eqs. (1) and (2)<sup>[152]</sup>. Thus, manure biochar is a viable option because it contains soluble  $PO_4^{3-}$  and  $CO_3^{2-}$ , which promote the precipitation of heavy metals and enhance its adsorption capacity<sup>[153]</sup>. For instance, Cao et al.<sup>[154]</sup> observed an increase in  $Pb$  phosphate precipitates on a bovine manure biochar's surface, accompanied by a decrease in  $PO_4^{3-}$ . This suggests that  $Pb(II)$  was removed via the formation of  $Pb$  phosphate precipitates on the biochar.



### Ion exchange

Ion exchange is an adsorption mechanism in which exchangeable cations present on the surface of biochar, such as  $H^+$ ,  $Na^+$ ,  $K^+$ ,  $Ca^{2+}$ , and  $Mg^{2+}$ , are replaced by heavy metal ions from wastewater. This process is primarily driven by the tendency of metal ions with higher charge densities and/or smaller hydration radii to replace these cations<sup>[155]</sup>. To enable this mechanism, the presence of both ion-binding sites, i.e., O-containing functional groups and exchangeable cations, is essential. Accordingly, biochar with these characteristics is highly conducive to facilitating ion exchange processes<sup>[156]</sup>.

### Surface complexation

Surface complexation involves the removal of heavy metals from a solution by forming multiatom complexes (inner- and outer-sphere complexes) between heavy metal ions and ligands<sup>[157]</sup>. Atoms such as S, N, and O in the functional groups act as ligands<sup>[158]</sup>. This indicates that the abundant O-containing groups, such as carboxyl and hydroxyl groups, on a biochar's surface can serve as adsorption sites for heavy metal ions<sup>[159]</sup>. These ligands act as electron donors, whereas the heavy metal ions function as electron acceptors<sup>[160]</sup>. This mechanism involves covalent or ionic coordination bonds between metal ions and surface ligands. Chemical binding (covalent bonding) leads to the formation of inner-sphere complexes, whereas electrostatic binding (ionic coordination) results in outer-sphere complexes<sup>[161]</sup>.

## Adsorption characteristics for different heavy metals

### Pb(II) adsorption

$Pb$  pollution is a global issue caused by mining, smelting, battery manufacturing, and industrial wastewater discharge. Despite these regulations, improper disposal of  $Pb$ -containing waste continues to contaminate water bodies and landfills. Global  $Pb$  production has increased by 232% in recent decades, reaching 11.3 million tons annually, contributing to widespread wastewater contamination<sup>[162]</sup>.  $Pb(II)$  is highly toxic and nonbiodegradable, posing serious health risks—particularly to children and pregnant women—and affecting multiple organ systems<sup>[85]</sup>. As such, regulatory agencies have established strict limits, with the World Health Organization (WHO) and the European Union permitting a maximum concentration of  $10 \mu g L^{-1}$  in drinking water<sup>[87,163]</sup>. Physicochemical treatment methods are commonly adopted to reduce  $Pb$  concentrations in wastewater. However, they are often associated with high costs, the generation of secondary waste, and the use of hazardous chemicals. Therefore, biochar has gained attention as a promising, low-cost, and environmentally friendly alternative for removing  $Pb(II)$  from wastewater. Therefore, numerous studies have investigated the adsorption of  $Pb(II)$  from aqueous solutions using animal manure biochar (Table 8).

The viability of animal manure biochar for  $Pb(II)$  adsorption was demonstrated by Xu et al.<sup>[164]</sup>. This research utilised biochar produced at  $500^\circ C$  from bovine manure and rice straw as adsorbents. To elucidate the adsorption mechanism of  $Pb(II)$  on biochar, surface analysis was performed, which revealed the formation of  $Pb$ -containing precipitates, such as  $PbCO_3$ ,  $Pb_3(CO_3)_2(OH)_2$ , and  $Pb_5(PO_4)_3Cl$ , after adsorption. These precipitates are attributed to the  $CO_3^{2-}$  and  $PO_4^{3-}$  originating from the inorganic constituents of the biochar. To further investigate the mechanism, the inorganic and organic fractions of the biochar were separated, and adsorption



**Table 8** Applications of animal manure biochar for adsorption of Pb(II)

Adsorbent	Pyrolysis and activation conditions	Surface area (m <sup>2</sup> g <sup>-1</sup> )	Total pore volume (cm <sup>3</sup> g <sup>-1</sup> )	Average pore diameter (nm)	Ash content (wt.%)	pH	H/C ratio	O/C ratio	Q <sub>max</sub> (mg g <sup>-1</sup> )	Ref.
Bovine	Biochar 500 °C for	150							101	[164]
Chicken	Biochar: 800 °C for 2 h				64.63	10.1	0.04	0.83	242.57	[166]
Chicken	Biochar: 550 °C for 2 h	7.09		7.09	87.2	9.95	0.06	0.49 <sup>a</sup>	120.383 <sup>b</sup>	[167]
Yak	Biochar: 350 °C for 2 h	6.36			23.91		1.2	0.55	155.36	[170]
	Activation: 10% H <sub>2</sub> O <sub>2</sub> solution at room temperature									
Bovine	Biochar: 300 °C for 4 h	25.94	0.055		27.13	9.98	0.15	0.92	175.53	[92]
	Activation: 2 M NaOH (shaking for 12 h at 65 °C)									
Swine	Biochar: 500 °C;								225.08	[52]
	Activation: Fe <sup>2+</sup> and Fe <sup>3+</sup> solutions (stirred for 20 min at 20–25 °C)									

<sup>a</sup> Calculated from the results of a proximate analysis of biochar; <sup>b</sup> The molecular weight of Pb(II) was assumed to be 207 g mol<sup>-1</sup>.

experiments were conducted on each fraction independently. The results showed that approximately 99% of Pb(II) adsorption was attributable to the inorganic fraction. Visual MINTEQ modelling confirmed that precipitation was the dominant mechanism. Bovine manure biochar exhibited a higher maximum adsorption capacity (101 mg g<sup>-1</sup>) than rice straw biochar (70 mg g<sup>-1</sup>), which was attributed to the higher carbonate and phosphate ion contents in bovine manure biochar. These findings indicate that animal manure biochar, particularly bovine manure biochar, is a highly effective adsorbent for removing Pb(II) from aqueous solutions.

Pyrolysis temperature plays a crucial role in determining the physicochemical properties of biochar, including its surface area, pore volume, and ash content<sup>[165]</sup>. These characteristics subsequently affect the adsorption capacity of biochar and the mechanisms of heavy metal removal. Yan et al.<sup>[166]</sup> demonstrated the effect of pyrolysis temperature on the adsorption performance of chicken manure biochar for removing Pb(II). The maximum adsorption capacity of Pb(II) increased with the pyrolysis temperature, reaching 242.57 mg g<sup>-1</sup> at 800 °C. The adsorption data fitted the Langmuir isotherm model better than the Freundlich model, indicating that Pb(II) adsorption follows a monolayer and is primarily driven by chemical interactions. Considering that the functional groups on the biochar decreased with an increase in pyrolysis temperature while the ash content increased, ion exchange and precipitation appear to be the dominant mechanisms of Pb(II) removal (Fig. 8). The role of precipitation has been demonstrated in bovine manure biochar. In the case of ion exchange, Zhao et al.<sup>[167]</sup> demonstrated its effectiveness by releasing alkaline metals, specifically Ca<sup>2+</sup> and Mg<sup>2+</sup>, when chicken manure biochar was used as an adsorbent for Pb(II).

Biochar produced at high pyrolysis temperatures typically shows an increased surface area, microporosity, and ash content<sup>[165]</sup>. Studies have confirmed that the adsorption of Pb(II) is enhanced by increasing the pyrolysis temperature. However, the high energy demand for increasing the pyrolysis temperatures highlights the necessity for low-temperature alternatives owing to their energy efficiency and economic feasibility<sup>[168]</sup>. However, biochar produced at low temperatures typically exhibits a relatively low surface porosity<sup>[169]</sup>. Numerous studies have explored enhancing the Pb(II) adsorption capacity at low pyrolysis temperatures by activating biochar with oxidising agents, alkalis, or acids. Wang & Liu<sup>[170]</sup> reported that yak manure biochar activated using an oxidising agent serves as an adsorbent for Pb(II). To modify the yak manure biochar, H<sub>2</sub>O<sub>2</sub> was employed, and the pyrolysis process was conducted at 350 °C. Following modification, the adsorption capacity of Pb(II) increased to 169.57 mg g<sup>-1</sup>, which was more than double that of pristine yak manure biochar. Additionally, the contents of O and carboxyl groups in yak manure biochar increased by 63.4% and 101%, respectively, whereas the ash content decreased by 42%. The reduction in the ash content after H<sub>2</sub>O<sub>2</sub> modification led to diminished Pb precipitation, whereas the increased number of O-containing functional groups facilitated complexation, which became the dominant removal mechanism. This was further supported by the better fit of the yak manure biochar data to the pseudo-second-order kinetic model, indicating the involvement of inner-sphere complexation<sup>[171]</sup>. These findings suggest that H<sub>2</sub>O<sub>2</sub>-modified biochar can serve as an effective surface sorbent for removing heavy metals from aqueous solutions.

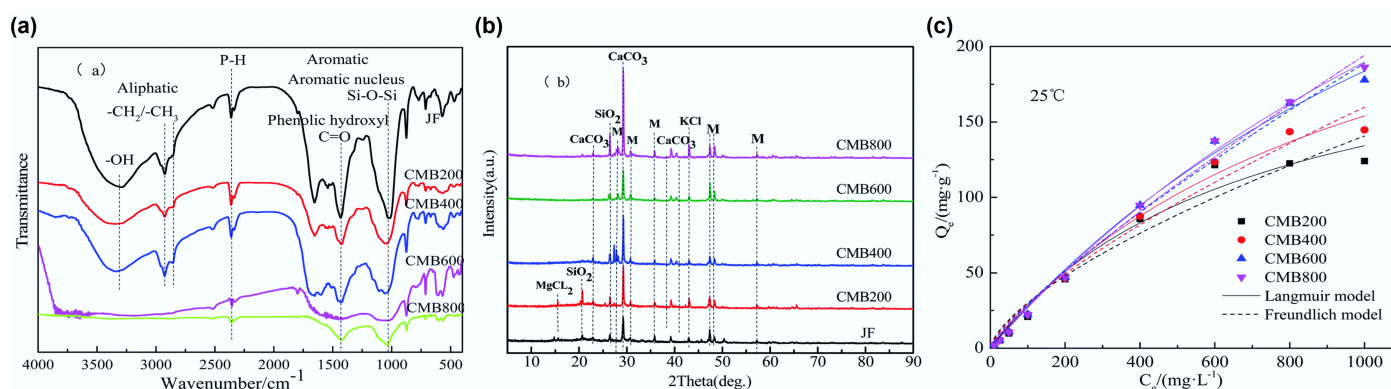


**Fig. 8** (a) FT-IR and (b) XRD spectra of chicken manure biochar and as a function of temperature and (c) their adsorption isotherm curves. Reprinted from Yan et al.<sup>[166]</sup> with permission. Copyright 2019 Royal Society of Chemistry

Chen et al.<sup>[92]</sup> investigated the effectiveness of alkaline activation for Pb(II) adsorption using bovine manure biochar. The biochar, pyrolysed at 300 °C and subsequently activated with sodium hydroxide (NaOH), showed a significant increase in adsorption capacity, reaching 175.53 mg g<sup>-1</sup>, compared with 51.32 mg g<sup>-1</sup> for the pristine bovine manure biochar. The alkaline treatment process led to an increase in the specific surface area, ion-exchange capacity, and abundance of O-containing functional groups. The adsorption equilibrium data fitted the Langmuir isotherm model, indicating the dominance of monolayer adsorption via chemical mechanisms. Additionally, the formation of Pb precipitates (2Pb(CO<sub>3</sub>)-Pb(OH)) and the complexation of Pb(II) with carboxyl and hydroxyl functional groups were detected on the biochar's surface. These findings demonstrate that alkaline activation significantly improves the Pb(II) adsorption capacity of bovine manure biochar.

In Wang et al.<sup>[52]</sup>, the surface area of iron-doped swine manure biochar (magnetic biochar, 225.08 m<sup>2</sup> g<sup>-1</sup>) was higher than that of pristine biochar and acid/base-activated biochar, which provided more adsorption sites. After the magnetic treatment, iron oxide was introduced into the biochar, thus increasing the ash content and providing additional electrostatic adsorption sites and precipitation ability<sup>[172]</sup>. Consequently, the adsorption capacity for Pb(II) increased from 30.02 to 95.94 L mg<sup>-1</sup>. Additionally, they found that the adsorption rate of magnetic biochar was higher than that of acid/base-activated biochar. Although metal/metal oxide-impregnated animal manure biochar has a higher adsorption capacity for heavy metals than most crop residue biochars, few studies have focused on this approach.

In short, for unmodified manure biochars, precipitation with carbonate and phosphate ions is the main driving force for Pb(II) adsorption, supplemented by ion exchange with alkaline earth metals. Therefore, higher pyrolysis temperatures further increase the adsorption capacity, peaking at 800 °C, where ion exchange and precipitation became dominant because of the increased ash content. For modified manure biochars, surface complexation with O-containing functional groups becomes the dominant mechanism, with H<sub>2</sub>O<sub>2</sub> or NaOH promoting precipitation and functional group complexation by improving surface area, ion exchange capacity, and O-containing functional groups. In metal-impregnated biochars, electrostatic attraction and metal oxide-assisted precipitation play a more significant role. Pb(II) removal was pronounced for biochar produced at high temperatures followed by Fe-based activation. Given that high-temperature production is energy-intensive and Fe activation requires additional treatment and chemicals, the production method should be selected according to the operational context. For commercial activated carbon and zeolite, the maximum adsorption capacities were 42.50 and 109.89 mg g<sup>-1</sup>,

respectively. Despite their high surface areas, both materials exhibited lower adsorption capacities than manure biochar. In particular, zeolite, even when produced from coal fly ash, showed inferior performance compared with manure biochar, indicating that manure biochar has a superior Pb(II) adsorption capacity.

### Cu(II) adsorption

Cu(II) ions are hazardous pollutants frequently present at high concentrations in industrial wastewater because of their extensive use in sectors such as electroplating, metal finishing, fertiliser production, mining, petroleum refining, and agrichemicals. Owing to its high toxicity, even at low concentrations, Cu(II) must be removed from wastewater to mitigate serious environmental and health risks, including gastrointestinal, liver, kidney, and respiratory disorders, neurotoxicity, and increased cancer risk. In aquatic ecosystems, excessive Cu(II) disrupts osmoregulatory mechanisms in freshwater organisms and may induce mutagenesis in humans. Regulatory agencies such as the USA Environmental Protection Agency have established strict Cu(II) concentration limits of 1.3 mg L<sup>-1</sup> for drinking water and as low as 0.25 mg L<sup>-1</sup> for industrial effluents<sup>[88,89]</sup>. Various removal technologies have been developed, including membrane filtration, electrodialysis, photocatalysis, and adsorption. Among these, adsorption is considered particularly promising because of its operational simplicity, cost-effectiveness, and broad applicability. Animal manure biochar is a viable candidate owing to its mineral-rich composition and low cost. Thus, investigations into the Cu(II) adsorption performance of animal manure biochar have been conducted to support practical applications. Adsorption results from previous studies are presented in Table 9.

Zhang et al.<sup>[173]</sup> investigated the mechanisms of Cu(II) adsorption onto bovine manure biochar produced at temperatures ranging from 300 to 700 °C. Notably, the maximum adsorption capacity for Cu(II) was achieved using biochar produced at 600 °C, reaching 70.54 mg g<sup>-1</sup>. The study found that the dominant mechanisms were ion exchange and precipitation, which accounted for 93.75%–97.01% of the total Cu(II) removal. Ion exchange was confirmed by the release of K<sup>+</sup>, Ca<sup>2+</sup>, and Mg<sup>2+</sup> ions from the biochar's surface. Indeed, the ion exchange capacity and the corresponding adsorption values decreased with an increase in the pyrolysis temperature owing to thermal stabilisation of the exchangeable metal. Additionally, surface complexation and cation- $\pi$  interactions contributed minimally (< 5%) and declined further at higher temperatures through the loss of functional groups and polarity. In contrast, precipitation became more significant at higher pyrolysis temperatures, which was facilitated by the increased ash content containing phosphate and carbonate. This was further supported by the detection of Cu precipitates, such as Cu<sub>3</sub>(PO<sub>4</sub>)<sub>2</sub> and Cu<sub>3</sub>(CO<sub>3</sub>)<sub>2</sub>(OH)<sub>2</sub>, as indicated by shifts in the phosphate and carbonate bands on the

**Table 9** Applications of animal manure biochar for the adsorption of Cu(II)

Adsorbent	Pyrolysis and activation conditions	Surface area (m <sup>2</sup> g <sup>-1</sup> )	Total pore volume (cm <sup>3</sup> g <sup>-1</sup> )	Ash content (wt.%)	pH	H/C ratio	O/C ratio	Q <sub>max</sub> (mg g <sup>-1</sup> )	Ref.
Bovine	Biochar: 300 °C for 1 h	3.42	0.0005	34.54	8.62	1.07	0.37	61.68	[173]
Bovine	Biochar: 400 °C for 1 h	3.66	0.0008	39.98	9.86	0.82	0.4	64.23	[173]
Bovine	Biochar: 500 °C for 1 h	4.34	0.0007	46.97	10.75	0.54	0.37	58.86	[173]
Bovine	Biochar: 600 °C for 1 h	6.11	0.0019	48.84	10.79	0.33	0.3	70.42	[173]
Bovine	Biochar: 700 °C for 1 h	10.61	0.004	50.45	10.83	0.29	0.26	66.77	[173]
Bovine	Biochar: 500 °C for 4 h	195.1	0.09	7.16 <sup>a</sup>	9.86	0.05		49.57 <sup>b</sup>	[153]
Yak	Biochar: 350 °C for 2 h	1.18		40.8		1.88	0.23	46.71	[170]
Yak	Biochar: 350 °C for 2 h; Activation: 10% H <sub>2</sub> O <sub>2</sub> solution at room temperature	6.36		23.91		1.2	0.55	64.98	[170]

<sup>a</sup> Sum of inorganic elements such as Ca, K, Mg, and Na in the biochar; <sup>b</sup> The molecular weight of Cu(II) was assumed to be 63.55 g mol<sup>-1</sup>.

biochar's surface. Overall, these findings indicate that precipitation and ion exchange are the primary mechanisms of Cu(II) adsorption by bovine manure biochar, particularly at elevated pyrolysis temperatures. These findings are supported by Lei et al.<sup>[153]</sup>, who reported that ion exchange contributed 39.2% to Cu(II) removal according to the release of Ca(II) from manure-derived biochar. Additionally, Visual MINTEQ modelling estimated that 50.0%–88.9% of the removed Cu(II) resulted from precipitation with carbonate, phosphate, and hydroxyl groups on the biochar's surface.

Because of the energy-intensive nature of pyrolysis, studies have investigated the activation of animal manure biochar produced at lower temperatures to enhance its adsorption capacity. Wang & Liu<sup>[170]</sup> investigated the adsorption capacity of Cu(II) using yak manure biochar pyrolysed at 350 °C and activated with H<sub>2</sub>O<sub>2</sub>. The activated biochar enhanced the adsorption capacity for Cu(II) from 45.96 to 71.39 mg g<sup>-1</sup> by increasing the O content and carboxylic functional groups on the biochar's surface, while reducing the ash content. Following adsorption, a shift in the C=O peak was observed in the FT-IR spectra, indicating the formation of metal–carboxyl complexes. Additionally, the formation of Cu–phosphate or Cu–carbonate precipitates decreased. These results suggest that H<sub>2</sub>O<sub>2</sub> activation effectively shifts the dominant Cu(II) removal mechanism from inorganic precipitation to surface complexation with carboxylic groups. Surface activation alters the surface properties, shifts the dominant adsorption mechanism, and enhances the adsorption capacity, suggesting that the adsorption of Cu(II) is not limited to a single mechanism.

In short, in unmodified biochars produced at medium to high temperatures, ion exchange with alkaline earth and alkali metals (e.g., Ca<sup>2+</sup>, Mg<sup>2+</sup>, K<sup>+</sup>) and precipitation with carbonate and phosphate species in the ash dominate, often accounting for over 90% of Cu(II) removal. In contrast, low-temperature biochars or oxidatively activated biochars exhibit a shift in the dominant mechanism toward surface complexation with O-containing functional groups, particularly carboxyl groups, while the contribution from precipitation decreases. These findings suggest that high-temperature pyrolysis should be prioritised when maximising precipitation-driven removal is desired, whereas low-temperature production combined with surface oxidation is more suitable when targeting complexation-driven adsorption for enhanced selectivity and functional group utilisation. Commercial activated carbon and zeolite showed maximum adsorption capacities of 15.0 and 57.80 mg g<sup>-1</sup>, respectively. Although commercial activated carbon had a high surface area, its Cu(II) removal efficiency was lower than that of manure biochar. Zeolite also exhibited a slightly lower adsorption capacity than manure biochar despite the higher surface area, further highlighting the effectiveness of manure biochar for adsorbing Cu(II).

### Cd(II) adsorption

Cd is widely distributed in the water, soil, and air owing to its natural sources, such as forest fires and volcanic eruptions, and anthropogenic

activities, including electroplating, battery manufacturing, pigment production, and metallurgy. As a persistent Group 1 carcinogen, Cd poses a significant threat to human health and ecosystems<sup>[90]</sup>. It bioaccumulates in living organisms and enters the human body through the food chain, leading to severe health outcomes such as nephrotoxicity, hepatotoxicity, bone demineralisation, endocrine disruption, reproductive disorders, and cancer, with chronic exposure leading to Itai-Itai disease<sup>[174,175]</sup>. Recognising its toxicity, the WHO has established a stringent drinking water limit of 3 µg L<sup>-1</sup><sup>[90]</sup>. Conventional Cd removal methods are often hindered by high operating costs and complex processes<sup>[91]</sup>. This has led to the exploration of low-cost and efficient alternatives, such as biochar, for treating wastewater. In this context, animal manure-derived biochar has attracted considerable attention for its potential to adsorb heavy metals. To demonstrate the practical potential of animal manure biochar, its Cd(II) adsorption performance has been widely investigated. Relevant findings from previous research are summarized in Table 10.

Huang et al.<sup>[156]</sup> examined the adsorption mechanisms of Cd(II) from aqueous solutions using chicken manure biochar pyrolysed at various temperatures. High-temperature biochar (700 °C) exhibited enhanced Cd(II) adsorption, achieving 149.55 mg g<sup>-1</sup>. Surface complexation and precipitation accounted for 92.4%–98.8% of Cd(II) adsorption. Surface complexation involves O-containing functional groups such as –COOH and –OH, whereas precipitation occurs through the formation of CdCO<sub>3</sub>, Cd<sub>3</sub>(PO<sub>4</sub>)<sub>2</sub>, and Cd<sub>5</sub>(PO<sub>4</sub>)<sub>3</sub>OH on the biochar's surface. Indeed, the ash content and P availability increased at higher pyrolysis temperatures. Consequently, precipitation (70%) was the dominant mechanism of surface complexation (22%) during Cd(II) adsorption.

These findings highlight the significance of precipitation in the adsorption of Cd(II) and emphasise the crucial roles of carbonate and phosphate present on the biochar's surface. This result is consistent with the findings of Idrees et al.<sup>[176]</sup>, who demonstrated that manure-derived biochar effectively adsorbed Cd(II). Their study compared the adsorption performance of poultry and farmyard manure biochar, and reported that poultry manure biochar exhibited a higher adsorption capacity, reaching 90.09 mg g<sup>-1</sup>. Despite its lower specific surface area, the improved adsorption performance of poultry manure biochar was attributed to its higher ash content, indicating that the process was primarily governed by chemical mechanisms. This interpretation is further supported by the adsorption behaviour, which follows pseudo-second-order kinetics and is a characteristic of chemisorption. In addition, the detection of CdCO<sub>3</sub> and Cd(OH)<sub>2</sub> on the biochar's surface suggested that precipitation played a significant role in the overall adsorption process.

Given the limitations of optimisation, the activation of manure biochar was explored to enhance its adsorption performance. Wang & Liu<sup>[170]</sup> studied Cd(II) adsorption by yak manure biochar activated with H<sub>2</sub>O<sub>2</sub>. Activation increased the number of O-containing func-

**Table 10** Applications of animal manure biochar the for adsorption of Cd(II)

Adsorbent	Pyrolysis and activation conditions	Surface area (m <sup>2</sup> g <sup>-1</sup> )	Ash content (wt. %)	pH	H/C ratio	O/C ratio	Q <sub>max</sub> (mg g <sup>-1</sup> )	Ref.
Chicken	Biochar: 300 °C for 4 h	4.51	40.09	9.68	0.94	0.38	62.55	[156]
Chicken	Biochar: 500 °C for 4 h	8.08	50	11.02	0.37	0.39	64.62	[156]
Chicken	Biochar: 700 °C for 4 h	10.89	54.78	11.81	0.17	0.36	123.16	[156]
Farmyard	Biochar: 450 °C for 5 h	10.11	27.18	8.2	0.056	0.37	60.94	[176]
Poultry	Biochar: 450 °C for 5 h	8.61	31.44	7.8	0.076	0.35	90.09	[176]
Yak	Biochar: 350 °C for 2 h	1.18	40.8		1.88	0.23	47.181	[170]
Yak	Biochar: 350 °C for 2 h; Activation: 10% H <sub>2</sub> O <sub>2</sub> solution at room temperature	6.36	23.91		1.2	0.55	69.08	[170]

tional groups and reduced the ash content on the biochar's surface. These changes enhanced Cd(II) affinity as the newly introduced functional groups acted as adsorption sites. Consequently, the dominant adsorption mechanism shifted from precipitation to surface complexation. Accordingly, the adsorption capacity for Pb(II) increased from 48.21 to 82.95 mg g<sup>-1</sup>. These findings indicate that Cd(II) adsorption does not rely on a single specific mechanism but depends on the availability of adsorption sites on the biochar's surface.

Overall, precipitation with carbonate and phosphate species in the ash fraction and surface complexation with O-containing functional groups such as –COOH and –OH are the main contributors for the adsorption of Cd(II). In unmodified biochars produced at high temperatures, precipitation dominates, resulting from the increased ash content and enhanced availability of phosphate and carbonate. In contrast, oxidative activation at lower pyrolysis temperatures reduces the ash content while enriching the surface functional groups, thereby shifting the dominant mechanism toward surface complexation. This mechanistic shift allows for greater functional group utilisation and improved selectivity. However, according to experimental results, as the adsorption of Cd(II) is primarily governed by precipitation, manure biochar produced at high temperatures is more advantageous. Commercial activated carbon and zeolite showed maximum adsorption capacities of 69.10 and 53.48 mg g<sup>-1</sup>, respectively. This highlights the effectiveness of manure biochar for the adsorption of Cd(II).

### Multi-metal adsorption

Heavy metals frequently coexist in industrial wastewater, leading to competitive interactions between the available adsorption sites on biochar's surface. This competition affects their ability to access and bind to the biochar's surface and is influenced by its inherent properties, such as hydration energy, hydrated ionic radius, and electronegativity<sup>[177]</sup>.

Under appropriate pH conditions, heavy metals exist as hydrated cations and their adsorption is closely related to their hydration characteristics. Metal ions with lower hydration energies shed their hydration shells more readily and exist as free cations, increasing their accessibility to adsorption sites<sup>[178]</sup>. Similarly, a smaller hydrated radius enhances the ability of metal ions to diffuse into biochar's pores and interact with functional groups on the surface<sup>[179]</sup>. For instance, Pb(II) (hydration energy: –1,481 kJ mol<sup>-1</sup>; hydrated radius: 0.401 nm), which has a lower hydration energy and smaller radius, consistently shows a higher affinity for these surface groups than Cd(II) or Zn(II), which have higher hydration energies and larger radii (Table 11)<sup>[180]</sup>. However, the hydration properties alone do not fully explain their adsorption behaviour, particularly with animal manure biochar. Kołodyńska et al.<sup>[171]</sup> demonstrated that the adsorption capacity of bovine manure biochar followed the order Pb(II) > Cu(II) > Cd(II). Interestingly, despite its higher hydration energy, Cu(II) showed greater adsorption than Cd(II), suggesting that other factors such as electronegativity and affinity for specific functional groups play critical roles.

The interactions between heavy metal ions and biochar are strongly influenced by their electronegativity and Lewis acid characteristics. Metal ions with higher electronegativity, such as Pb(II), tend to exhibit stronger electrostatic interactions with the negatively charged O-containing functional groups on the biochar's surface. Notably, the electronegativity of heavy metal ions followed the order Pb (2.33) > Cu (1.90) > Cd (1.69)<sup>[54]</sup>. In the case of Lewis acid–base interactions, Pb(II), a hard Lewis acid, exhibits a strong affinity for hard base functional groups such as carboxyl and hydroxyl groups, resulting in higher adsorption compared with

softer acids such as Cd(II)<sup>[170]</sup>. Additionally, in precipitation, the affinity of metal ions for anionic components (PO<sub>4</sub><sup>3-</sup> and CO<sub>3</sub><sup>2-</sup>) plays a critical role in the adsorption performance. Among the divalent metals, Pb(II) has the highest affinity for PO<sub>4</sub><sup>3-</sup>, followed by Cu(II), Cd(II), and Ni(II). These factors highlight the importance of the inherent properties of metal ions in determining the dominant adsorption mechanisms of biochar.

In multi-metal systems, competition among metal ions reduces the overall adsorption capacity and alters the dominant adsorption mechanism. For instance, Wang & Liu<sup>[170]</sup> found that the Pb(II) adsorption capacity of yak manure biochar decreased from 77.17 mg g<sup>-1</sup> in single-metal systems to 35.42 mg g<sup>-1</sup> in multi-metal systems due to competition. Xu et al.<sup>[147]</sup> reported a similar 21.5% reduction using bovine manure biochar. Despite these considerations, Pb(II) exhibited the highest adsorption capacity, which was attributed to its pronounced affinity for phosphate and carbonate groups, with precipitation remaining the dominant removal mechanism. For Cu(II), the presence of Pb(II) in multi-metal systems further reduced its adsorption capacity from 26.58 mg g<sup>-1</sup> in single-metal solutions to 21.33 mg g<sup>-1</sup> in multi-metal solutions<sup>[147]</sup>. Xu et al.<sup>[170]</sup> reported a 46.5% reduction in Cu(II) adsorption in multi-metal systems. Cu(II) removal remained balanced between precipitation and surface complexation. However, the dominance of Pb(II) binding to shared adsorption sites likely reduced the contribution of precipitation to Cu(II). The removal of Cd(II) was most adversely affected by competitive adsorption. Its larger hydrated radii and lower electronegativities hinder access to adsorption sites. In particular, Cd(II) removal efficiency decreased by 100% in multi-metal systems compared with single-metal systems. The preferential adsorption of Pb(II) and Cu(II) through strong interactions with O-containing functional groups and mineral components hindered the adsorption of Cd(II) onto the available active sites.

These findings highlight the importance of considering the surface characteristics of biochar and the intrinsic properties of individual metal ions when designing and applying biochar-based adsorption systems for wastewater treatment. In multi-metal systems, heavy metal adsorption is governed by the complex physicochemical properties of the adsorbate. In the presence of Pb(II), Cu(II), and Cd(II), the adsorption of Cd(II) is notably hindered by competitive interactions. Therefore, understanding these competitive dynamics is essential for designing effective biochar treatment strategies. Recently, studies have applied machine learning models to predict multi-metal adsorption performance. For instance, Castillo et al.<sup>[183]</sup> developed a  $q_{e,r}$ -based artificial neural network (ANN) model to simulate and predict the adsorption of multi-metals [Cd(II), Ni(II), Zn(II), and Cu(II)] in bone char-based water treatment systems. Similarly, Hanandeh et al.<sup>[184]</sup> demonstrated that a generalised regression neural network (GRNN) model could capture the physical constraints of multi-metal [Pb(II), Cu(II), and Ni(II)] adsorption systems using date seed biochar, enabling generalisable predictions. On the basis of the models, the key parameters influencing the adsorption capacity of manure biochar can be identified and elucidate the primary mechanisms governing multi-metal adsorption. However, research on multi-metal adsorption by

**Table 11** Hydration energy, hydrated ionic radius, and electronegativity of heavy metal cations<sup>[181,182]</sup>

Heavy metal ion	Pb(II)	Cu(II)	Cd(II)	Zn(II)
Hydration energy (kJ mol <sup>-1</sup> )	–1,481	–2,100	–1,807	–2,046
Hydrated ionic radius (nm)	0.401	0.419	0.426	0.430
Electronegativity	2.330	1.900	1.690	1.650



manure-derived biochar remains scarce. To address this gap, future studies should employ machine learning-based modelling approaches to predict and optimise the multi-metal adsorption performance of manure biochar.

## Simultaneous adsorption of organic contaminants and heavy metals

In wastewater treatment, the coexistence of organic and inorganic pollutants is common. Therefore, it is imperative to assess the capacity of manure-derived biochar for the simultaneous adsorption of coexisting organic and inorganic contaminants. Jiang et al.<sup>[185]</sup> investigated the use of biochar derived from swine manure digestate (SMD) for the treatment of livestock breeding wastewater, which typically contains both heavy metals and antibiotics. The study particularly evaluated the adsorption efficiency of a contaminant mixture, including zinc (Zn), copper (Cu), arsenic (As), sulfadimidine, and tylosin, using modified SMD biochar. Notably, KMnO<sub>4</sub>-modified SMD biochar exhibited the highest removal performance, with removal efficiencies of 48.96% for Zn, 66.53% for Cu, 83.98% for As, 83.76% for sulfadimidine, and 77.34% for tylosin. These results demonstrate that the abundance of surface functional groups and surface charge properties of modified SMD biochar facilitated the simultaneous adsorption of both heavy metals and antibiotics. Despite its potential, the simultaneous treatment of complex mixtures of heavy metals and organic contaminants using manure-derived biochar has rarely been explored. Moreover, as with multi-metal adsorption, competitive interactions among the coexisting contaminants have been reported to reduce the overall adsorption efficiency. Thus, further studies are needed to validate the performance of manure-derived biochar under mixed pollutant conditions and to elucidate the underlying mechanisms governing competitive adsorption for practical applications in wastewater treatment.

## Management of spent manure-derived biochar

For sustainable adsorption practices, the recycling of biochar should be prioritised, with chemical desorption, particularly using NaOH, being the most common approach<sup>[186,187]</sup>. However, the intrinsic properties and functionalities of manure-derived biochar may change during chemical recycling, necessitating in-depth research to evaluate these alterations. In addition, the use of chemical reagents raises concerns about potential secondary pollution, which has prompted interest in alternative applications. Given the nutrient-rich composition of manure-derived biochar, alternative applications such as phytoremediation could be explored<sup>[188]</sup>. However, because of concerns regarding the leaching of adsorbed contaminants, comprehensive long-term leaching tests should be conducted. Nevertheless, as spent biochar inherently poses the risk of releasing hazardous substances, it should be managed appropriately to prevent environmental pollution. Safe disposal options include incineration and isolation in lined landfills. Incineration serves as a final disposal method, often integrated into waste-to-energy systems, where the spent adsorbents can partly substitute for solid fuel as a thermal energy source<sup>[189]</sup>. Although organic pollutants are decomposed into CO<sub>2</sub> during combustion, chlorine-containing compounds in dyes can lead to the formation of dioxins, posing environmental risks<sup>[190]</sup>. Landfilling is another final disposal method. However, because the heavy metals in biochar may leach during the acidic phase of landfill conditions, the lining must ensure complete containment of the biochar. At present, research on

the feasibility and environmental safety of these disposal methods for spent manure-derived biochar remains scarce, highlighting the need for further investigation.

## Conclusions and perspectives

### Advantages of using animal manure biochar

Animal manure biochar offers distinct physicochemical advantages over conventional lignocellulosic biochar, making it a promising candidate for advanced wastewater treatment. Unlike conventional lignocellulosic biochar, manure-derived biochar is inherently rich in inorganic minerals, such as Ca, Mg, K, P, and trace metals. These elements serve as active sites for ion exchange and contribute to the formation of metal precipitates (e.g., phosphates and carbonates) during adsorption, thereby enhancing the removal efficiency of heavy metals. Additionally, the N content originating from the feedstock improves surface reactivity and enables functionalisation with amino groups. The presence of O-containing functional groups (e.g., -COOH, -OH, and =O) on the biochar's surface facilitates electrostatic interactions, hydrogen bonding, and complexation with cationic and anionic pollutants. Furthermore, the graphitised C structures and aromatic domains formed at elevated pyrolysis temperatures promote  $\pi$ - $\pi$  electron donor-acceptor interactions, which are particularly important for the adsorption of recalcitrant organic compounds such as dyes and antibiotics. Moreover, various activation methods such as physical oxidation, acid/alkali treatments, and metal impregnation can be applied to improve the porosity and surface chemistry, further improving the adsorption capacity and selectivity. Owing to these properties, animal manure biochar exhibited a higher adsorption capacity than commercial activated carbon and zeolite for the adsorption of heavy metals despite the lower surface area of manure biochar. This highlights the versatility and effectiveness of animal manure biochar as an adsorbent for removing various pollutants from wastewater, demonstrating its potential for practical application in wastewater treatment.

In addition to its adsorption performance, production cost is a critical factor for the practical application of manure-derived biochar. Several techno-economic assessments have reported that the production cost of swine manure biochar is approximately 193 USD ton<sup>-1</sup>, whereas that of bovine manure biochar is around 237 USD ton<sup>-1</sup><sup>[191,192]</sup>. These values are substantially lower than those for biochars derived from lignocellulosic biomass, such as forest residues (1,044–1,600 USD ton<sup>-1</sup>), orchard biomass (448–1,846 USD ton<sup>-1</sup>), and wood (474–704 USD ton<sup>-1</sup>)<sup>[193–195]</sup>. In addition, the price of commercial activated carbon is 450 USD ton<sup>-1</sup><sup>[196]</sup>. The cost-effectiveness of manure-derived biochar primarily stems from the minimal raw material costs, as animal manure is an abundantly available byproduct of livestock production. In some cases, its utilisation can even offset manure disposal expenses, further reducing the raw material costs. Moreover, manure biochar production can be directly integrated into existing manure management systems at livestock facilities, thereby minimising transportation and handling expenses. These factors collectively position manure-derived biochar as an economically viable and resource-efficient alternative to adsorbents derived from lignocellulosic biomass.

### Limitations and future directions

Despite its potential, several limitations must be addressed to enable the large-scale application of animal manure biochar in water treatment. A key challenge lies in the heterogeneity of the feedstocks' composition. Specifically, variations in animal species, diet, bedding materials, and collection methods affect the organic and inorganic



contents of manure, leading to inconsistencies in the physicochemical properties of the resulting biochar<sup>[197,198]</sup>. Additionally, the insufficient number of adsorption sites, including heteroatoms and functional groups, in animal manure biochar restricts its adsorption capacity. Although lower pyrolysis temperatures preserve these surface functionalities, the resulting biochar has inadequate porosity. Furthermore, given the complex mixture of inorganic and organic pollutants released from industrial sources, pollutant removal via adsorption can be hindered by the competition among coexisting substances<sup>[181,199]</sup>. Although several studies have reported the high adsorption capacity of biochar under controlled laboratory conditions, limited data are available on its long-term stability, regeneration capacity, and practical field-scale applications. In addition, natural aging progressively alters its surface properties, pore structure, and functional groups, highlighting the need for research on its long-term stability, including its adsorption capacity and release of contaminants. Economic considerations, including activation costs and the regeneration or disposal of spent biochar, have also received limited attention. These factors should be integrated into future research to establish biochar as a cost-effective and practical wastewater treatment material.

Several critical issues must be addressed before animal manure biochar can be practically applied as an adsorbent in wastewater treatment. To address issues arising from the heterogeneity of the manure, future research should prioritise the development of standardised protocols for feedstock preparation and pyrolysis to ensure reproducibility and consistent adsorption capacity. This can be achieved by conducting year-scale studies using manure from a consistent livestock facility to ensure a uniform feedstock. Additionally, surface modification strategies are essential to enrich the biochar's surface with pores and functional groups, which can be achieved through advanced activation methods such as sequential chemical and physical treatments. To overcome pollutant competition in complex wastewaters, biochar must be engineered for multifunctionality and selectivity by incorporating metal oxides, functional ligands, or nanomaterials that enable the removal of contaminants. Their long-term performance, including the structural stability and the release of contaminants, must be evaluated under realistic operational conditions. Advancing such research would facilitate the formulation of effective pollution control strategies by providing a basis for determining the optimal reapplication intervals, maintenance protocols, and the overall economic viability of using biochar. Sustainable and cost-effective regeneration methods, such

as low-temperature thermal treatment or mild chemical washing, should be explored to promote the reuse of spent biochar. Finally, pilot-scale studies and field demonstrations are imperative to validate the laboratory-scale results, optimise the operational parameters, and facilitate the practical implementation of biochar in real-world wastewater treatment systems.

## Conclusions

Animal manure biochar is an emerging eco-friendly adsorbent with significant potential for addressing agricultural waste valorisation and wastewater treatment challenges. Its abundance of mineral phases (e.g., carbonate, phosphate) and reactive functional groups (e.g.,  $-\text{COOH}$ ,  $-\text{OH}$ ) supports diverse adsorption mechanisms, including electrostatic interactions,  $\pi$ - $\pi$  EDA interactions, hydrogen bonding, ion exchange, surface complexation, and mineral precipitation. This review summarises recent advances in the use of animal manure-derived biochar for removing dyes, antibiotics, and heavy metals, emphasising adsorption mechanisms and offering pollutant-specific optimisation strategies. Optimisation strategies for various pollutants are summarised in Table 12.

For dyes, unmodified manure biochars remove cationic species mainly via electrostatic attraction above the  $\text{pH}_{\text{pzc}}$  and anionic species via protonation-driven attraction under acidic conditions, with  $\pi$ - $\pi$  EDA interactions and hydrogen bonding serving as secondary mechanisms. Sheep manure biochar generally shows superior performance because of its high surface area and O/C ratio, whereas alkali metal modification enhances adsorption by increasing the porosity and the amount of O-containing groups, and enabling additional ion exchange pathways. Thus, enhancing the O-containing groups through targeted modification should be prioritised to achieve higher adsorption capacity.

For antibiotics, the adsorption mechanisms vary according to their molecular properties. Owing to the high oxygen content of TC, its adsorption is predominantly governed by interactions with functional groups. Therefore, surface modification (e.g.,  $\text{H}_3\text{PO}_4$  treatment) is required to introduce the O-containing functional groups onto the surface of the manure-derived biochar. The removal of LEV involves multiple chemical and physical interactions, while adsorption of CIP is governed primarily by hydrogen bonding and  $\pi$ - $\pi$  EDA interactions. Consequently, biochar's properties should be tailored to the specific characteristics of each antibiotic.

For heavy metals, high-temperature biochars ( $> 600^\circ\text{C}$ ) promote precipitation with carbonate and phosphate species and ion

**Table 12** Summary of adsorption mechanisms, performance-enhancing factors, and optimisation strategies of animal manure-derived biochar for dyes, antibiotics, and heavy metals

Pollutant type	Dominant adsorption mechanism	Performance-enhancing factor	Optimisation strategy
Dyes	<ul style="list-style-type: none"> <li>Cationic species: electrostatic attraction above <math>\text{pH}_{\text{pzc}}</math></li> <li>Anionic species: protonation-driven attraction under acidic conditions</li> <li><math>\pi</math>-<math>\pi</math> EDA interactions, hydrogen bonding</li> </ul>	<ul style="list-style-type: none"> <li>High surface area and porosity</li> <li>High O-containing groups and O/C ratio</li> <li>Alkali metal modification for ion exchange</li> </ul>	<ul style="list-style-type: none"> <li>Enhance O-containing groups via targeted modification</li> </ul>
Antibiotics	<ul style="list-style-type: none"> <li>TC: <math>\text{pH}</math> 3.5–8.0 (zwitterionic form), hydrogen bonding in addition to <math>\pi</math>-<math>\pi</math> EDA interactions</li> <li>LEV: Multilayer (physical) adsorption involving electrostatic attraction, hydrogen bonding, cation-<math>\pi</math>, and <math>\pi</math>-<math>\pi</math> EDA interactions, and pore filling</li> <li>CIP: monolayer (chemical) adsorption by hydrogen bonding between <math>-\text{O}</math>, <math>-\text{F}</math>, and <math>-\text{N}</math> of CIP and O-containing sites; <math>\pi</math>-<math>\pi</math> EDA interactions enhanced by higher aromaticity</li> </ul>	<ul style="list-style-type: none"> <li>TC: surface area, enriched O-containing functional groups</li> <li>LEV: porosity and surface area</li> <li>CIP: surface area and O-containing sites</li> </ul>	<ul style="list-style-type: none"> <li>Enhance O-containing groups via targeted modification for TC and CIP</li> <li>Increase the pyrolysis temperature to enhance the surface area for LEV</li> </ul>
Heavy metals	<ul style="list-style-type: none"> <li>Precipitation with carbonate and phosphate species</li> <li>Ion exchange with alkali/alkaline earth metals</li> <li>Surface complexation with O-containing functional groups</li> </ul>	<ul style="list-style-type: none"> <li>Ash content with carbonate and phosphate species</li> <li>O-containing functional groups</li> </ul>	<ul style="list-style-type: none"> <li>Raise the pyrolysis temperature</li> <li>Establish a balance between adsorption performance and energy-economic trade-offs for the activation treatments</li> </ul>

exchange with alkali/alkaline earth metals, enabling high removal efficiency for Pb(II), Cu(II), and Cd(II). When activated, low-temperature biochars can achieve adsorption capacities similar to those of unmodified high-temperature biochars. However, activation introduces additional processing steps, thereby increasing the overall production costs. Accordingly, an optimal balance between adsorption performance and the energy-economic trade-offs of such intensive treatments should be established.

Overall, owing to the intrinsic characteristics of manure, a reliable adsorption performance of manure-derived biochar for dyes and heavy metals [Pb(II), Cu(II), Cd(II)] can be achieved via simple pyrolysis. For removing antibiotics, however, effective adsorption requires tailored pyrolysis and activation conditions because of the distinct properties of each antibiotic. The utilisation of manure-derived biochars can address two key objectives: mitigating environmental pollution through improved manure management and producing effective adsorbents for advanced wastewater treatment. In conclusion, this resource-efficient strategy holds considerable promise for advancing circular economy principles and promoting sustainable manure management.

## Author contributions

The authors confirm their contributions to the paper as follows: study conception and design, manuscript revision: Lee S, Kim M, Park G, Jung S, Kwon EE; draft manuscript preparation: Lee S; material preparation, data collection and analysis: Kim M, Park G; validation, data curation: Jung S; review, editing, supervision, and conceptual guidance: Kwon EE. All authors reviewed the results and approved the final version of the manuscript.

## Data availability

The datasets used or analysed during the current study are available from the corresponding author upon reasonable request.

## Funding

This work was supported by the National Research Foundation of Korea (NRF) grant funded by the Korean Government (MSIT) (grant number: RS-2023-NR077231).

## Declarations

### Conflict of interest

The authors declare that they have no conflict of interest.

### Author details

<sup>1</sup>Department of Earth Resources and Environmental Engineering, Hanyang University, Seoul 04763, Republic of Korea; <sup>2</sup>Department of Environmental Engineering, Kyungpook National University, Daegu 41566, Republic of Korea

## References

- [1] Young SL, Frongillo EA, Jamaluddine Z, Melgar-Quinonez H, Pérez-Escamilla R, et al. 2021. Perspective: the importance of water security for ensuring food security, good nutrition, and well-being. *Advances in Nutrition* 12:1058–1073
- [2] Meese AF, Kim DJ, Wu X, Le L, Napier C, et al. 2022. Opportunities and challenges for industrial water treatment and reuse. *ACS ES&T Engineering* 2:465–488
- [3] Ramesh B, Saravanan A, Senthil Kumar P, Yaashikaa PR, Thamarai P, et al. 2023. A review on algae biosorption for the removal of hazardous pollutants from wastewater: Limiting factors, prospects and recommendations. *Environmental Pollution* 327:121572
- [4] Nishshanka GKSH, Thevarajah B, Nimarshana PHV, Prajapati SK, Ariyadasa TU. 2023. Real-time integration of microalgae-based bioremediation in conventional wastewater treatment plants: Current status and prospects. *Journal of Water Process Engineering* 56:104248
- [5] Intisar A, Ramzan A, Hafeez S, Hussain N, Irfan M, et al. 2023. Adsorptive and photocatalytic degradation potential of porous polymeric materials for removal of pesticides, pharmaceuticals, and dyes-based emerging contaminants from water. *Chemosphere* 336:139203
- [6] Haciosmanoğlu GG, Mejías C, Martín J, Santos JL, Aparicio I, et al. 2022. Antibiotic adsorption by natural and modified clay minerals as designer adsorbents for wastewater treatment: A comprehensive review. *Journal of Environmental Management* 317:115397
- [7] Kuncoro EP, Mitha Isnadina DR, Darmokoeseomo H, Dzembaramatiny F, Kusuma HS. 2018. Characterization and isotherm data for adsorption of Cd<sup>2+</sup> from aqueous solution by adsorbent from mixture of bagasse-bentonite. *Data in Brief* 16:354–360
- [8] Saini K, Singh J, Malik S, Saharan Y, Goyat R, et al. 2024. Metal-organic frameworks: a promising solution for efficient removal of heavy metal ions and organic pollutants from industrial wastewater. *Journal of Molecular Liquids* 399:124365
- [9] Kumar N, Pandey A, Rosy, Sharma YC. 2023. A review on sustainable mesoporous activated carbon as adsorbent for efficient removal of hazardous dyes from industrial wastewater. *Journal of Water Process Engineering* 54:104054
- [10] Luo J, Fu K, Yu D, Hristovski KD, Westerhoff P, et al. 2021. Review of advances in engineering nanomaterial adsorbents for metal removal and recovery from water: synthesis and microstructure impacts. *ACS ES&T Engineering* 1:623–661
- [11] Ewis D, Ba-Abbad MM, Benamor A, El-Naas MH. 2022. Adsorption of organic water pollutants by clays and clay minerals composites: a comprehensive review. *Applied Clay Science* 229:106686
- [12] Mian MM, Ao W, Deng S. 2023. Sludge-based biochar adsorbent: Pore tuning mechanisms, challenges, and role in carbon sequestration. *Biochar* 5:83
- [13] Berazneva J, Woolf D, Lee DR. 2021. Local lignocellulosic biofuel and biochar co-production in Sub-Saharan Africa: the role of feedstock provision in economic viability. *Energy Economics* 93:105031
- [14] Jia W, Qin W, Zhang Q, Wang X, Ma Y, et al. 2018. Evaluation of crop residues and manure production and their geographical distribution in China. *Journal of Cleaner Production* 188:954–965
- [15] Qiu M, Liu L, Ling Q, Cai Y, Yu S, et al. 2022. Biochar for the removal of contaminants from soil and water: a review. *Biochar* 4:19
- [16] Alegbeleye OO, Sant'Ana AS. 2020. Manure-borne pathogens as an important source of water contamination: an update on the dynamics of pathogen survival/transport as well as practical risk mitigation strategies. *International Journal of Hygiene and Environmental Health* 227:113524
- [17] Wang M, Cao W, Sun C, Sun Z, Miao Y, et al. 2019. To distinguish the primary characteristics of agro-waste biomass by the principal component analysis: an investigation in East China. *Waste Management* 90:100–120
- [18] Xie S, Zhang T, You S, Mukherjee S, Pu M, et al. 2025. Applied machine learning for predicting the properties and carbon and phosphorus fate of pristine and engineered hydrochar. *Biochar* 7:19
- [19] Yan C, Li J, Sun Z, Wang X, Xia S. 2024. Mechanistic insights into removal of pollutants in adsorption and advanced oxidation processes by livestock manure derived biochar: a review. *Separation and Purification Technology* 346:127457
- [20] Chen X, Wu B, Yang W, Zhao G, Han J, et al. 2023. Biochar as a multi-functional material facilitate the organohalide remediation: a state-of-the-art review. *Chemical Engineering Journal* 460:141700
- [21] OECD and Food and Agriculture Organization of the United Nations. 2021. *OECD-FAO Agricultural Outlook 2021–2030*. Paris, France: Organisation for Economic Co-operation and Development (OECD). doi: 10.1787/19428846-en
- [22] Food and Agriculture Organization of the United Nations. 2019. *Livestock manure*. Roma, Italy: FAO. [www.fao.org/faostat/en/#data/EMN](http://www.fao.org/faostat/en/#data/EMN)

- [23] Liu Z, Wang X. 2020. Manure treatment and utilization in production systems. In *Animal Agriculture*, ed. Bazer FW, Lamb GC, Wu G. Cambridge: Academic Press. pp. 455–467 doi: [10.1016/B978-0-12-817052-6.00026-4](https://doi.org/10.1016/B978-0-12-817052-6.00026-4)
- [24] Leitner S, Ring D, Wanyama GN, Korir D, Pelster DE, et al. 2021. Effect of feeding practices and manure quality on CH<sub>4</sub> and N<sub>2</sub>O emissions from uncovered cattle manure heaps in Kenya. *Waste Management* 126:209–220
- [25] Liu Q, He X, Luo G, Wang K, Li D. 2022. Deciphering the dominant components and functions of bacterial communities for lignocellulose degradation at the composting thermophilic phase. *Bioresource Technology* 348:126808
- [26] Trabue SL, Kerr BJ, Scoggins KD, Andersen D, van Weelden M. 2021. Swine diets impact manure characteristics and gas emissions: Part I protein level. *Science of The Total Environment* 755:142528
- [27] Su X, Zhang T, Zhao J, Mukherjee S, Alotaibi NM, et al. 2024. Phosphorus fraction in hydrochar from co-hydrothermal carbonization of swine manure and rice straw: an optimization analysis based on response surface methodology. *Water* 16:2208
- [28] Guo Z, Zhang J, Fan J, Yang X, Yi Y, et al. 2019. Does animal manure application improve soil aggregation? Insights from nine long-term fertilization experiments. *Science of The Total Environment* 660:1029–1037
- [29] Foong SY, Liew RK, Lee CL, Tan WP, Peng W, et al. 2022. Strategic hazard mitigation of waste furniture boards via pyrolysis: Pyrolysis behavior, mechanisms, and value-added products. *Journal of Hazardous Materials* 421:126774
- [30] Li J, Cao L, Yuan Y, Wang R, Wen Y, et al. 2018. Comparative study for microcystin-LR sorption onto biochars produced from various plant- and animal-wastes at different pyrolysis temperatures: Influencing mechanisms of biochar properties. *Bioresource Technology* 247:794–803
- [31] Leng L, Xiong Q, Yang L, Li H, Zhou Y, et al. 2021. An overview on engineering the surface area and porosity of biochar. *Science of The Total Environment* 763:144204
- [32] Iwuozor KO, Emenike EC, Omonayin EO, Bamigbola JO, Ojo HT, et al. 2023. Unlocking the hidden value of pods: A review of thermochemical conversion processes for biochar production. *Bioresource Technology Reports* 22:101488
- [33] Yin G, Zhang F, Gao Y, He W, Zhang Q, et al. 2023. Increase of bio-char yield by adding potassium salt during biomass pyrolysis. *Journal of the Energy Institute* 110:101342
- [34] Bikane K, Yu J, Long X, Paterson N, Millan M. 2020. Linking char reactivity to structural and morphological evolution during high pressure pyrolysis of Morupule coal. *Chemical Engineering Science: X* 8:100072
- [35] Wang S, Zhang H, Huang H, Xiao R, Li R, et al. 2020. Influence of temperature and residence time on characteristics of biochars derived from agricultural residues: a comprehensive evaluation. *Process Safety and Environmental Protection* 139:218–229
- [36] Lee J, Sarmah AK, Kwon EE. 2019. Production and formation of biochar. In *Biochar from Biomass and Waste*, ed. Ok YS, Tsang DCW, Bolan N, Novak JM. Amsterdam: Elsevier. pp. 3–18 doi: [10.1016/b978-0-12-811729-3.00001-7](https://doi.org/10.1016/b978-0-12-811729-3.00001-7)
- [37] Safdari MS, Amini E, Weise DR, Fletcher TH. 2019. Heating rate and temperature effects on pyrolysis products from live wildland fuels. *Fuel* 242:295–304
- [38] Ighalo JO, Iwuchukwu FU, Eyankware OE, Iwuozor KO, Olotu K, et al. 2022. Flash pyrolysis of biomass: a review of recent advances. *Clean Technologies and Environmental Policy* 24:2349–63
- [39] Qambrani NA, Rahman MM, Won S, Shim S, Ra C. 2017. Biochar properties and eco-friendly applications for climate change mitigation, waste management, and wastewater treatment: A review. *Renewable and Sustainable Energy Reviews* 79:255–273
- [40] Shafizadeh A, Rastegari H, Shahbeik H, Mobli H, Pan J, et al. 2023. A critical review of the use of nanomaterials in the biomass pyrolysis process. *Journal of Cleaner Production* 400:136705
- [41] Selvanathan M, Yann KT, Chung CH, Selvarajoo A, Arumugasamy SK, et al. 2017. Adsorption of copper(II) ion from aqueous solution using biochar derived from rambutan (*Nephelium lappaceum*) peel: feed-forward neural network modelling study. *Water, Air, & Soil Pollution* 228:299
- [42] Akhil D, Lakshmi D, Kartik A, Vo DVN, Arun J, et al. 2021. Production, characterization, activation and environmental applications of engineered biochar: a review. *Environmental Chemistry Letters* 19:2261–2297
- [43] Panwar NL, Pawar A. 2022. Influence of activation conditions on the physicochemical properties of activated biochar: a review. *Biomass Conversion and Biorefinery* 12:925–947
- [44] Rajapaksha AU, Chen SS, Tsang DCW, Zhang M, Vithanage M, et al. 2016. Engineered/designer biochar for contaminant removal/immobilization from soil and water: Potential and implication of biochar modification. *Chemosphere* 148:276–291
- [45] Lopez-Tenllado FJ, Motta IL, Hill JM. 2021. Modification of biochar with high-energy ball milling: Development of porosity and surface acid functional groups. *Bioresource Technology Reports* 15:100704
- [46] Shu T, Lu P, He N. 2013. Mercury adsorption of modified mulberry twig chars in a simulated flue gas. *Bioresource Technology* 136:182–187
- [47] Sizmur T, Fresno T, Akgül G, Frost H, Moreno-Jiménez E. 2017. Biochar modification to enhance sorption of inorganics from water. *Bioresource Technology* 246:34–47
- [48] Venkatachalam CD, Sekar S, Sengottian M, Ravichandran SR, Bhuvaneshwaran P. 2023. A critical review of the production, activation, and morphological characteristic study on functionalized biochar. *Journal of Energy Storage* 67:107525
- [49] Shahib II, Iftikhar J, Oyekunle DT, Elkhilfi Z, Jawad A, et al. 2022. Influences of chemical treatment on sludge derived biochar: Physico-chemical properties and potential sorption mechanisms of lead (II) and methylene blue. *Journal of Environmental Chemical Engineering* 10:107725
- [50] Li B, Li K. 2019. Effect of nitric acid pre-oxidation concentration on pore structure and nitrogen/oxygen active decoration sites of ethylenediamine -modified biochar for mercury(II) adsorption and the possible mechanism. *Chemosphere* 220:28–39
- [51] Hasegawa G, Deguchi T, Kanamori K, Kobayashi Y, Kageyama H, et al. 2015. High-level doping of nitrogen, phosphorus, and sulfur into activated carbon monoliths and their electrochemical capacitances. *Chemistry of Materials* 27:4703–4712
- [52] Wang RZ, Huang DL, Zhang C, Liu YG, Zeng GM, et al. 2019. Insights into the effect of chemical treatment on the physicochemical characteristics and adsorption behavior of pig manure-derived biochars. *Environmental Science and Pollution Research* 26:1962–1972
- [53] Anthonysamy SI, Lahijani P, Mohammadi M, Mohamed AR. 2022. Alkali-modified biochar as a sustainable adsorbent for the low-temperature uptake of nitric oxide. *International Journal of Environmental Science and Technology* 19:7127–7140
- [54] Uchimiya M, Lima IM, Thomas Klasson K, Chang S, Wartelle LH, et al. 2010. Immobilization of heavy metal ions (CuII, CdII, NiII, and PbII) by broiler litter-derived biochars in water and soil. *Journal of Agricultural and Food Chemistry* 58:5538–5544
- [55] Chen W, Gong M, Li K, Xia M, Chen Z, et al. 2020. Insight into KOH activation mechanism during biomass pyrolysis: Chemical reactions between O-containing groups and KOH. *Applied Energy* 278:115730
- [56] Han Z, Sani B, Mroziak W, Obst M, Beckingham B, et al. 2015. Magnetite impregnation effects on the sorbent properties of activated carbons and biochars. *Water Research* 70:394–403
- [57] Liu Y, Sohi SP, Liu S, Guan J, Zhou J, et al. 2019. Adsorption and reductive degradation of Cr(VI) and TCE by a simply synthesized zero valent iron magnetic biochar. *Journal of Environmental Management* 235:276–281
- [58] Zhang Y, Liu N, Yang Y, Li J, Wang S, et al. 2020. Novel carbothermal synthesis of Fe, N co-doped oak wood biochar (Fe/N-OB) for fast and effective Cr(VI) removal. *Colloids and Surfaces A: Physicochemical and Engineering Aspects* 600:124926
- [59] Han Y, Cao X, Ouyang X, Sohi SP, Chen J. 2016. Adsorption kinetics of magnetic biochar derived from peanut hull on removal of Cr (VI) from



- aqueous solution: Effects of production conditions and particle size. *Chemosphere* 145:336–341
- [60] Shi M, Min X, Ke Y, Lin Z, Yang Z, et al. 2021. Recent progress in understanding the mechanism of heavy metals retention by iron (oxyhydr)oxides. *Science of the Total Environment* 752:141930
- [61] Alhashimi HA, Aktas CB. 2017. Life cycle environmental and economic performance of biochar compared with activated carbon: A meta-analysis. *Resources, Conservation and Recycling* 118:13–26
- [62] Hadjittofi L, Prodromou M, Pashalidis I. 2014. Activated biochar derived from cactus fibres—Preparation, characterization and application on Cu(II) removal from aqueous solutions. *Bioresource Technology* 159:460–464
- [63] Iriarte-Velasco U, Sierra I, Zudaire L, Ayastuy JL. 2016. Preparation of a porous biochar from the acid activation of pork bones. *Food and Bioproducts Processing* 98:341–353
- [64] Zhang C, Li Y, Shen H, Shuai D. 2021. Simultaneous coupling of photocatalytic and biological processes: a promising synergistic alternative for enhancing decontamination of recalcitrant compounds in water. *Chemical Engineering Journal* 403:126365
- [65] Wang Y, Gao Q, You Q, Liao G, Xia H, et al. 2016. Porous polyimide framework: a novel versatile adsorbent for highly efficient removals of azo dye and antibiotic. *Reactive and Functional Polymers* 103:9–16
- [66] Wang CC, Li JR, Lv XL, Zhang YQ, Guo G. 2014. Photocatalytic organic pollutants degradation in metal–organic frameworks. *Energy & Environmental Science* 7:2831–2867
- [67] Choudhary S, Sharma K, Kumar V, Sharma V. 2024. RSM-CCD directed modeling and optimization of a low-cost adsorbent based on sodium dodecyl sulfate for the selective removal of malachite green and methylene blue dyes: Kinetics, isotherm, and thermodynamics analysis. *Microchemical Journal* 205:111158
- [68] Wang Y, Zhang H, Chen L. 2011. Ultrasound enhanced catalytic ozonation of tetracycline in a rectangular air-lift reactor. *Catalysis Today* 175:283–292
- [69] Al-Jabari MH, Sulaiman S, Ali S, Barakat R, Mubarak A, et al. 2019. Adsorption study of levofloxacin on reusable magnetic nanoparticles: Kinetics and antibacterial activity. *Journal of Molecular Liquids* 291:111249
- [70] Peng X, Hu F, Zhang T, Qiu F, Dai H. 2018. Amine-functionalized magnetic bamboo-based activated carbon adsorptive removal of ciprofloxacin and norfloxacin: A batch and fixed-bed column study. *Bioresource Technology* 249:924–934
- [71] McVotto F, Wei Q, Macharia DK, Huang M, Shen C, et al. 2021. Effect of dye structure on color removal efficiency by coagulation. *Chemical Engineering Journal* 405:126674
- [72] Kishor R, Purchase D, Saratale GD, Romanholo Ferreira LF, Hussain CM, et al. 2021. Degradation mechanism and toxicity reduction of methyl orange dye by a newly isolated bacterium *Pseudomonas aeruginosa* MZ520730. *Journal of Water Process Engineering* 43:102300
- [73] Sharma G, Sharma S, Kumar A, Naushad M, Du B, et al. 2019. Honeycomb structured activated carbon synthesized from *Pinus roxburghii* cone as effective bioadsorbent for toxic malachite green dye. *Journal of Water Process Engineering* 32:100931
- [74] Oladoye PO, Ajiboye TO, Wanyonyi WC, Omotola EO, Oladipo ME. 2023. Ozonation, electrochemical, and biological methods for the remediation of malachite green dye wastewaters: a mini review. *Sustainable Chemistry for the Environment* 3:100033
- [75] Saya L, Malik V, Gautam D, Gambhir G, Balendra, et al. 2022. A comprehensive review on recent advances toward sequestration of levofloxacin antibiotic from wastewater. *Science of The Total Environment* 813:152529
- [76] Han CH, Park HD, Kim SB, Yargeau V, Choi JW, et al. 2020. Oxidation of tetracycline and oxytetracycline for the photo-Fenton process: Their transformation products and toxicity assessment. *Water Research* 172:115514
- [77] Leichtweis J, Vieira Y, Welter N, Silvestri S, Dotto GL, et al. 2022. A review of the occurrence, disposal, determination, toxicity and remediation technologies of the tetracycline antibiotic. *Process Safety and Environmental Protection* 160:25–40
- [78] Kayani KF. 2025. Tetracycline in the environment: Toxicity, uses, occurrence, detection, and removal by covalent organic frameworks – Recent advances and challenges. *Separation and Purification Technology* 364:132418
- [79] Zhang H, Quan H, Yin S, Sun L, Lu H. 2022. Unraveling the toxicity associated with ciprofloxacin biodegradation in biological wastewater treatment. *Environmental Science & Technology* 56:15941–15952
- [80] Mahmoud MAM, Abdel-Mohsein HS. 2019. Hysterical tetracycline in intensive poultry farms accountable for substantial gene resistance, health and ecological risk in Egypt- manure and fish. *Environmental Pollution* 255:113039
- [81] Oladoye PO, Ajiboye TO, Omotola EO, Oyewola OJ. 2022. Methylene blue dye: Toxicity and potential elimination technology from wastewater. *Results in Engineering* 16:100678
- [82] Waghchaure RH, Adole VA, Jagdale BS. 2022. Photocatalytic degradation of methylene blue, rhodamine B, methyl orange and Eriochrome black T dyes by modified ZnO nanocatalysts: a concise review. *Inorganic Chemistry Communications* 143:109764
- [83] Balasurya S, Okla MK, Mohebaldin A, Al-ghamdi AA, Abdel-Maksoud MA, et al. 2022. Self-assembling of 3D layered flower architecture of BiOI modified  $\text{MgCr}_2\text{O}_4$  nanosphere for wider spectrum visible-light photocatalytic degradation of rhodamine B and malachite green: Mechanism, pathway, reactive sites and toxicity prediction. *Journal of Environmental Management* 308:114614
- [84] Li S, Huang T, Du P, Liu W, Hu J. 2020. Photocatalytic transformation fate and toxicity of ciprofloxacin related to dissociation species: experimental and theoretical evidences. *Water Research* 185:116286
- [85] Saravanan P, Saravanan V, Rajeshkannan R, Arnica G, Rajasimman M, et al. 2024. Comprehensive review on toxic heavy metals in the aquatic system: sources, identification, treatment strategies, and health risk assessment. *Environmental Research* 258:119440
- [86] Zeng X, Xu X, Boezen HM, Huo X. 2016. Children with health impairments by heavy metals in an e-waste recycling area. *Chemosphere* 148:408–415
- [87] Chowdhury IR, Chowdhury S, Mazumder MAJ, Al-Ahmed A. 2022. Removal of lead ions ( $\text{Pb}^{2+}$ ) from water and wastewater: A review on the low-cost adsorbents. *Applied Water Science* 12:185
- [88] Mallik AK, Kabir SMF, Bin Abdur Rahman F, Sakib MN, Efty SS, et al. 2022. Cu(II) removal from wastewater using chitosan-based adsorbents: A review. *Journal of Environmental Chemical Engineering* 10:108048
- [89] Al-Saydeh SA, El-Naas MH, Zaidi SJ. 2017. Copper removal from industrial wastewater: A comprehensive review. *Journal of Industrial and Engineering Chemistry* 56:35–44
- [90] Zhang W, Xia L, Deen KM, Asselin E, Ma B, et al. 2023. Enhanced removal of cadmium from wastewater by electro-assisted cementation process: A peculiar Cd reduction on Zn anode. *Chemical Engineering Journal* 452:139692
- [91] Tan Y, Wan X, Ni X, Wang L, Zhou T, et al. 2022. Efficient removal of Cd (II) from aqueous solution by chitosan modified kiwi branch biochar. *Chemosphere* 289:133251
- [92] Chen ZL, Zhang JQ, Huang L, Yuan ZH, Li ZJ, et al. 2019. Removal of Cd and Pb with biochar made from dairy manure at low temperature. *Journal of Integrative Agriculture* 18:201–210
- [93] Xu D, Tan XL, Chen CL, Wang XK. 2008. Adsorption of Pb(II) from aqueous solution to MX-80 bentonite: Effect of pH, ionic strength, foreign ions and temperature. *Applied Clay Science* 41:37–46
- [94] Khormaei M, Nasernejad B, Edrisi M, Eslamzadeh T. 2007. Copper biosorption from aqueous solutions by sour orange residue. *Journal of Hazardous Materials* 149:269–274
- [95] Hu XJ, Liu YG, Zeng GM, You SH, Wang H, et al. 2014. Effects of background electrolytes and ionic strength on enrichment of Cd(II) ions with magnetic graphene oxide-supported sulfanilic acid. *Journal of Colloid and Interface Science* 435:138–144
- [96] Degen A, Kosec M. 2000. Effect of pH and impurities on the surface charge of zinc oxide in aqueous solution. *Journal of the European Ceramic Society* 20:667–673
- [97] Gaur VK, Sharma P, Sirohi R, Awasthi MK, Dussap CG, et al. 2020. Assessing the impact of industrial waste on environment and

- mitigation strategies: A comprehensive review. *Journal of Hazardous Materials* 398:123019
- [98] Dong W, Xing J, Chen Q, Huang Y, Wu M, et al. 2024. Hydrogen bonds between the oxygen-containing functional groups of biochar and organic contaminants significantly enhance sorption affinity. *Chemical Engineering Journal* 499:156654
- [99] Sullivan GL, Prigmore RM, Knight P, Godfrey AR. 2019. Activated carbon biochar from municipal waste as a sorptive agent for the removal of polyaromatic hydrocarbons (PAHs), phenols and petroleum based compounds in contaminated liquids. *Journal of Environmental Management* 251:109551
- [100] Ahmed MB, Zhou JL, Ngo HH, Johir MAH, Sun L, et al. 2018. Sorption of hydrophobic organic contaminants on functionalized biochar: Protagonist role of  $\pi$ - $\pi$  electron-donor-acceptor interactions and hydrogen bonds. *Journal of Hazardous Materials* 360:270–278
- [101] Stöhr M, Sadhukhan M, Al-Hamdani YS, Hermann J, Tkatchenko A. 2021. Coulomb interactions between dipolar quantum fluctuations in van der Waals bound molecules and materials. *Nature Communications* 12:137
- [102] Abdul G, Zhu X, Chen B. 2017. Structural characteristics of biochar-graphene nanosheet composites and their adsorption performance for phthalic acid esters. *Chemical Engineering Journal* 319:9–20
- [103] Tsui L, Roy WR. 2008. The potential applications of using compost chars for removing the hydrophobic herbicide atrazine from solution. *Bioresource Technology* 99:5673–5678
- [104] Dou S, Ke XX, Shao ZD, Zhong LB, Zhao QB, et al. 2022. Fish scale-based biochar with defined pore size and ultrahigh specific surface area for highly efficient adsorption of ciprofloxacin. *Chemosphere* 287:131962
- [105] Xing J, Dong W, Liang N, Huang Y, Wu M, et al. 2023. Sorption of organic contaminants by biochars with multiple porous structures: Experiments and molecular dynamics simulations mediated by three-dimensional models. *Journal of Hazardous Materials* 458:131953
- [106] Wei L, Huang Y, Huang L, Li Y, Huang Q, et al. 2020. The ratio of H/C is a useful parameter to predict adsorption of the herbicide metolachlor to biochars. *Environmental Research* 184:109324
- [107] Wang Z, Jang HM. 2022. Comparative study on characteristics and mechanism of levofloxacin adsorption on swine manure biochar. *Bioresource Technology* 351:127025
- [108] Civiš S, Lamanec M, Špirko V, Kubišta J, Špet'ko M, et al. 2023. Hydrogen bonding with hydridic hydrogen—Experimental low-temperature IR and computational study: is a revised definition of hydrogen bonding appropriate? *Journal of the American Chemical Society* 145:8550–8559
- [109] Chen J, Zhou J, Zheng W, Leng S, Ai Z, et al. 2024. A complete review on the oxygen-containing functional groups of biochar: Formation mechanisms, detection methods, engineering, and applications. *Science of the Total Environment* 946:174081
- [110] Lin Z, Jin L, Liu Y, Wang Y. 2023. Hydrogen bonding donor/acceptor active sites exposed on imide-functionalized carbon dots aid in enhancing arsenic adsorption performance. *Chemical Engineering Journal* 459:141540
- [111] Zhuo SN, Dai TC, Ren HY, Liu BF. 2022. Simultaneous adsorption of phosphate and tetracycline by calcium modified corn stover biochar: Performance and mechanism. *Bioresource Technology* 359:127477
- [112] Flórez E, Jimenez-Orozco C, Acelas N. 2024. Unravelling the influence of surface functional groups and surface charge on heavy metal adsorption onto carbonaceous materials: an in-depth DFT study. *Materials Today Communications* 39:108647
- [113] Kah M, Sigmund G, Xiao F, Hofmann T. 2017. Sorption of ionizable and ionic organic compounds to biochar, activated carbon and other carbonaceous materials. *Water Research* 124:673–692
- [114] Xiong J, Xu J, Zhou M, Zhao W, Chen C, et al. 2021. Quantitative characterization of the site density and the charged state of functional groups on biochar. *ACS Sustainable Chemistry & Engineering* 9:2600–2608
- [115] Reguyal F, Sarmah AK. 2018. Adsorption of sulfamethoxazole by magnetic biochar: Effects of pH, ionic strength, natural organic matter and 17 $\alpha$ -ethinylestradiol. *Science of The Total Environment* 628-629:722–730
- [116] Fan S, Wang Y, Wang Z, Tang J, Tang J, et al. 2017. Removal of methylene blue from aqueous solution by sewage sludge-derived biochar: Adsorption kinetics, equilibrium, thermodynamics and mechanism. *Journal of Environmental Chemical Engineering* 5:601–611
- [117] Zhao J, Gao F, Sun Y, Fang W, Li X, et al. 2021. New use for biochar derived from bovine manure for tetracycline removal. *Journal of Environmental Chemical Engineering* 9:105585
- [118] Zhang P, Li Y, Cao Y, Han L. 2019. Characteristics of tetracycline adsorption by cow manure biochar prepared at different pyrolysis temperatures. *Bioresource Technology* 285:121348
- [119] Salazar-Rabago JJ, Leyva-Ramos R, Rivera-Utrilla J, Ocampo-Perez R, Cerino-Cordova FJ. 2017. Biosorption mechanism of Methylene Blue from aqueous solution onto White Pine (*Pinus durangensis*) sawdust: Effect of operating conditions. *Sustainable Environment Research* 27:32–40
- [120] Wang H, Fang C, Wang Q, Chu Y, Song Y, et al. 2018. Sorption of tetracycline on biochar derived from rice straw and swine manure. *RSC Advances* 8:16260–16268
- [121] Shaha CK, Karmaker S, Saha TK. 2024. Efficient adsorptive removal of levofloxacin using sulfonated graphene oxide: Adsorption behavior, kinetics, and thermodynamics. *Heliyon* 10
- [122] Roca Jalil ME, Baschini M, Sapag K. 2015. Influence of pH and antibiotic solubility on the removal of ciprofloxacin from aqueous media using montmorillonite. *Applied Clay Science* 114:69–76
- [123] Yuan J, Wen Y, Dionysiou DD, Sharma VK, Ma X. 2022. Biochar as a novel carbon-negative electron source and mediator: electron exchange capacity (EEC) and environmentally persistent free radicals (EPFRs): a review. *Chemical Engineering Journal* 429:132313
- [124] Hu Y, Zhu Y, Zhang Y, Lin T, Zeng G, et al. 2019. An efficient adsorbent: Simultaneous activated and magnetic ZnO doped biochar derived from camphor leaves for ciprofloxacin adsorption. *Bioresource Technology* 288:121511
- [125] Noyes PD, Miranda D, Oliveira de Carvalho G, Perfetti-Bolaño A, Guida Y, et al. 2025. Climate change drives persistent organic pollutant dynamics in marine environments. *Communications Earth & Environment* 6:363
- [126] Ahmad A, Khan N, Giri BS, Chowdhary P, Chaturvedi P. 2020. Removal of methylene blue dye using rice husk, cow dung and sludge biochar: Characterization, application, and kinetic studies. *Bioresource Technology* 306:123202
- [127] Huang W, Chen J, Zhang J. 2018. Adsorption characteristics of methylene blue by biochar prepared using sheep, rabbit and pig manure. *Environmental Science and Pollution Research* 25:29256–29266
- [128] Yu J, Zhang X, Wang D, Li P. 2018. Adsorption of methyl orange dye onto biochar adsorbent prepared from chicken manure. *Water Science and Technology* 77:1303–1312
- [129] Lu Y, Chen J, Bai Y, Gao J, Peng M. 2019. Adsorption properties of methyl orange in water by sheep manure biochar. *Polish Journal of Environmental Studies* 28:3791–3797
- [130] Dilekoğlu MF. 2022. Malachite green adsorption from aqueous solutions onto biochar derived from sheep manure: Adsorption kinetics, isotherm, thermodynamic, and mechanism. *International Journal of Phytoremediation* 24:436–446
- [131] Sharma P, Sharma S, Sharma SK, Shao Y, Guo F, et al. 2024. Evaluation of optimized conditions for the adsorption of malachite green by SnO<sub>2</sub>-modified sugarcane bagasse biochar nanocomposites. *RSC Advances* 14:29201–29214
- [132] Wu Z, Zhang H, Ali E, Shahab A, Huang H, et al. 2023. Synthesis of novel magnetic activated carbon for effective Cr(VI) removal via synergistic adsorption and chemical reduction. *Environmental Technology & Innovation* 30:103092
- [133] Zhu Y, Yi B, Yuan Q, Wu Y, Wang M, et al. 2018. Removal of methylene blue from aqueous solution by cattle manure-derived low temperature biochar. *RSC Advances* 8:19917–19929
- [134] Hao H, Zhang Q, Qiu Y, Meng L, Wei X, et al. 2020. Insight into the degradation of Orange G by persulfate activated with biochar



- modified by iron and manganese oxides: Synergism between Fe and Mn. *Journal of Water Process Engineering* 37:101470
- [135] Wang K, Peng N, Sun J, Lu G, Chen M, et al. 2020. Synthesis of silica-composited biochars from alkali-fused fly ash and agricultural wastes for enhanced adsorption of methylene blue. *Science of the Total Environment* 729:139055
- [136] Kovalakova P, Cizmas L, McDonald TJ, Marsalek B, Feng M, et al. 2020. Occurrence and toxicity of antibiotics in the aquatic environment: A review. *Chemosphere* 251:126351
- [137] Yang Y, Cai S, Mo C, Dong J, Chen S, Wen Z. 2025. Profiles of antibiotic resistance risk in diverse water environments. *Communications Earth & Environment* 6:158
- [138] Adedeji OM, Jahan K. 2023. Removal of pollutants from aqueous product of Co-hydrothermal liquefaction: Adsorption and isotherm studies. *Chemosphere* 321:138165
- [139] He J, Xiao Y, Tang J, Chen H, Sun H. 2019. Persulfate activation with sawdust biochar in aqueous solution by enhanced electron donor-transfer effect. *Science of the Total Environment* 690:768–777
- [140] Huang W, Chen J, Zhang J. 2020. Removal of ciprofloxacin from aqueous solution by rabbit manure biochar. *Environmental Technology* 41:1380–1390
- [141] Gupta VK, Pathania D, Sharma S, Singh P. 2013. Preparation of bio-based porous carbon by microwave assisted phosphoric acid activation and its use for adsorption of Cr(VI). *Journal of Colloid and Interface Science* 401:125–132
- [142] Chen T, Luo L, Deng S, Shi G, Zhang S, et al. 2018. Sorption of tetracycline on H<sub>3</sub>PO<sub>4</sub> modified biochar derived from rice straw and swine manure. *Bioresource Technology* 267:431–437
- [143] Peng H, Gao P, Chu G, Pan B, Peng J, et al. 2017. Enhanced adsorption of Cu(II) and Cd(II) by phosphoric acid-modified biochars. *Environmental Pollution* 229:846–853
- [144] Qiu B, Tao X, Wang H, Li W, Ding X, et al. 2021. Biochar as a low-cost adsorbent for aqueous heavy metal removal: A review. *Journal of Analytical and Applied Pyrolysis* 155:105081
- [145] Barquilha CER, Braga MCB. 2021. Adsorption of organic and inorganic pollutants onto biochars: Challenges, operating conditions, and mechanisms. *Bioresource Technology Reports* 15:100728
- [146] Zhao Z, Wu Q, Nie T, Zhou W. 2019. Quantitative evaluation of relationships between adsorption and partition of atrazine in biochar-amended soils with biochar characteristics. *RSC Advances* 9:4162–4171
- [147] Xu X, Cao X, Zhao L. 2013. Comparison of rice husk- and dairy manure-derived biochars for simultaneously removing heavy metals from aqueous solutions: Role of mineral components in biochars. *Chemosphere* 92:955–961
- [148] Chin JF, Heng ZW, Teoh HC, Chong WC, Pang YL. 2022. Recent development of magnetic biochar crosslinked chitosan on heavy metal removal from wastewater – Modification, application and mechanism. *Chemosphere* 291:133035
- [149] Du B, Li W, Zhu H, Xu J, Wang Q, et al. 2023. A functional lignin for heavy metal ions adsorption and wound care dressing. *International Journal of Biological Macromolecules* 239:124268
- [150] Frišták V, Beliančinová K, Polřáková L, Moreno-Jiménez E, Zimmermann AR, et al. 2024. Engineered Mg-modified biochar-based sorbent for arsenic separation and pre-concentration. *Scientific Reports* 14:28680
- [151] Han R, Gao Y, Jia Y, Wang S. 2024. Heterogeneous precipitation behavior and mechanism during the adsorption of cationic heavy metals by biochar: roles of inorganic components. *Journal of Hazardous Materials* 480:136322
- [152] Xu X, Cao X, Zhao L, Wang H, Yu H, et al. 2013. Removal of Cu, Zn, and Cd from aqueous solutions by the dairy manure-derived biochar. *Environmental Science and Pollution Research* 20:358–368
- [153] Lei S, Shi Y, Qiu Y, Che L, Xue C. 2019. Performance and mechanisms of emerging animal-derived biochars for immobilization of heavy metals. *Science of The Total Environment* 646:1281–1289
- [154] Cao X, Ma L, Gao B, Harris W. 2009. Dairy-manure derived biochar effectively sorbs lead and atrazine. *Environmental Science & Technology* 43:3285–3291
- [155] Malhotra M, Puglia M, Kalluri A, Chowdhury D, Kumar CV. 2022. Adsorption of metal ions on graphene sheet for applications in environmental sensing and wastewater treatment. *Sensors and Actuators Reports* 4:100077
- [156] Huang F, Gao LY, Deng JH, Chen SH, Cai KZ. 2018. Quantitative contribution of Cd<sup>2+</sup> adsorption mechanisms by chicken-manure-derived biochars. *Environmental Science and Pollution Research* 25:28322–28334
- [157] Zhou Z, Zhang C, Xi M, Ma H, Jia H. 2023. Multi-scale modeling of natural organic matter-heavy metal cations interactions: Aggregation and stabilization mechanisms. *Water Research* 238:120007
- [158] Chang SH. 2022. Micro/nanomotors for metal ion detection and removal from water: A review. *Materials Today Sustainability* 19:100196
- [159] Wang F, Jin L, Guo C, Min L, Zhang P, et al. 2021. Enhanced heavy metals sorption by modified biochars derived from pig manure. *Science of The Total Environment* 786:147595
- [160] Zhu H, Chen S, Luo Y. 2023. Adsorption mechanisms of hydrogels for heavy metal and organic dyes removal: a short review. *Journal of Agriculture and Food Research* 12:100552
- [161] Yan Y, Wan B, Mansor M, Wang X, Zhang Q, et al. 2022. Co-sorption of metal ions and inorganic anions/organic ligands on environmental minerals: a review. *Science of The Total Environment* 803:149918
- [162] Jagaba AH, Lawal IM, Birniwa AH, Affam AC, Usman AK, et al. 2024. Sources of water contamination by heavy metals. In *Membrane Technologies for Heavy Metal Removal from Water*, ed. Jaafar J, Zaidi AA, Naseer MN. Boca Raton: CRC Press. pp. 3–27 doi: 10.1201/9781003326281
- [163] World Health Organization (WHO). 2021. *Lead in drinking-water. Switzerland*. [www.who.int/publications/i/item/9789240020863](http://www.who.int/publications/i/item/9789240020863)
- [164] Xu X, Cao X, Zhao L, Zhou H, Luo Q. 2014. Interaction of organic and inorganic fractions of biochar with Pb(II) ion: Further elucidation of mechanisms for Pb(II) removal by biochar. *RSC Advances* 4:44930–44937
- [165] Zhang X, Zheng H, Wu J, Chen W, Chen Y, et al. 2021. Physicochemical and adsorption properties of biochar from biomass-based pyrolytic polygeneration: Effects of biomass species and temperature. *Biochar* 3:657–670
- [166] Yan C, Xu Y, Wang L, Liang X, Sun Y, et al. 2020. Effect of different pyrolysis temperatures on physico-chemical characteristics and lead(II) removal of biochar derived from chicken manure. *RSC Advances* 10:3667–3674
- [167] Zhao M, Dai Y, Zhang M, Feng C, Qin B, et al. 2020. Mechanisms of Pb and/or Zn adsorption by different biochars: Biochar characteristics, stability, and binding energies. *Science of The Total Environment* 717:136894
- [168] Alcazar-Ruiz A, Silva LS, Dorado F. 2024. Economic viability assessment of bioenergy production from agroindustrial wastes through fast pyrolysis. *Energy* 311:133441
- [169] Acharya BS, Dodla S, Wang JJ, Pavuluri K, Darapuneni M, et al. 2024. Biochar impacts on soil water dynamics: knowns, unknowns, and research directions. *Biochar* 6:34
- [170] Wang Y, Liu R. 2018. H<sub>2</sub>O<sub>2</sub> treatment enhanced the heavy metals removal by manure biochar in aqueous solutions. *Science of The Total Environment* 628-629:1139–1148
- [171] Kołodyńska D, Wnętrzak R, Leahy JJ, Hayes MHB, Kwapiński W, et al. 2012. Inert and adsorptive characterization of biochar in metal ions removal. *Chemical Engineering Journal* 197:295–305
- [172] Zhang A, Li X, Xing J, Xu G. 2020. Adsorption of potentially toxic elements in water by modified biochar: a review. *Journal of Environmental Chemical Engineering* 8:104196
- [173] Zhang P, Zhang X, Yuan X, Xie R, Han L. 2021. Characteristics, adsorption behaviors, Cu(II) adsorption mechanisms by cow manure biochar derived at various pyrolysis temperatures. *Bioresource Technology* 331:125013
- [174] Saravanan A, Kumar PS, Vo DVN, Swetha S, Nguen PT, et al. 2021. Ultrasonic assisted agro waste biomass for rapid removal of Cd(II) ions from aquatic environment: mechanism and modelling analysis. *Chemosphere* 271:129484

- [175] Peng ZD, Lin XM, Zhang YL, Hu Z, Yang XJ, et al. 2021. Removal of cadmium from wastewater by magnetic zeolite synthesized from natural, low-grade molybdenum. *Science of The Total Environment* 772:145355
- [176] Idrees M, Batool S, Hussain Q, Ullah H, Al-Wabel MI, et al. 2016. High-efficiency remediation of cadmium ( $\text{Cd}^{2+}$ ) from aqueous solution using poultry manure- and farmyard manure-derived biochars. *Separation Science and Technology* 51:2307–2317
- [177] Pan J, Gao B, Guo K, Gao Y, Xu X, et al. 2022. Insights into selective adsorption mechanism of copper and zinc ions onto biogas residue-based adsorbent: Theoretical calculation and electronegativity difference. *Science of The Total Environment* 805:150413
- [178] Wan S, Wu J, Zhou S, Wang R, Gao B, et al. 2018. Enhanced lead and cadmium removal using biochar-supported hydrated manganese oxide (HMO) nanoparticles: Behavior and mechanism. *Science of The Total Environment* 616–617:1298–1306
- [179] Guan X, Yuan X, Zhao Y, Bai J, Li Y, et al. 2022. Adsorption behaviors and mechanisms of Fe/Mg layered double hydroxide loaded on bentonite on Cd (II) and Pb (II) removal. *Journal of Colloid and Interface Science* 612:572–583
- [180] Cheng S, Liu Y, Xing B, Qin X, Zhang C, et al. 2021. Lead and cadmium clean removal from wastewater by sustainable biochar derived from poplar saw dust. *Journal of Cleaner Production* 314:128074
- [181] Ni BJ, Huang QS, Wang C, Ni TY, Sun J, et al. 2019. Competitive adsorption of heavy metals in aqueous solution onto biochar derived from anaerobically digested sludge. *Chemosphere* 219:351–357
- [182] Mahmoud AED, Al-Qahtani KM, Alfaij SO, Al-Qahtani SF, Alsamhan FA. 2021. Green copper oxide nanoparticles for lead, nickel, and cadmium removal from contaminated water. *Scientific Reports* 11:12547
- [183] Mendoza-Castillo DI, Reynel-Ávila HE, Sánchez-Ruiz FJ, Trejo-Valencia R, Jaime-Leal JE, et al. 2018. Insights and pitfalls of artificial neural network modeling of competitive multi-metallic adsorption data. *Journal of Molecular Liquids* 251:15–27
- [184] El Hanandeh A, Mahdi Z, Imtiaz MS. 2021. Modelling of the adsorption of Pb, Cu and Ni ions from single and multi-component aqueous solutions by date seed derived biochar: Comparison of six machine learning approaches. *Environmental Research* 192:110338
- [185] Jiang B, Lin Y, Mbog JC. 2018. Biochar derived from swine manure digestate and applied on the removals of heavy metals and antibiotics. *Bioresource Technology* 270:603–611
- [186] Priyanka, Wood IE, Al-Gailani A, Kolosz BW, Cheah KW, et al. 2024. Cleaning up metal contamination after decades of energy production and manufacturing: reviewing the value in use of biochars for a sustainable future. *Sustainability* 16:8838
- [187] Diao Y, Shan R, Li M, Gu J, Yuan H, et al. 2023. Efficient adsorption of a sulfonamide antibiotic in aqueous solutions with N-doped magnetic biochar: Performance, mechanism, and reusability. *ACS Omega* 8:879–892
- [188] Sharma S, Bolan S, Mukherjee S, Petruzzelli G, Pedron F, et al. 2025. Role of organic and biochar amendments on enhanced bioremediation of soils contaminated with persistent organic pollutants (POPs). *Current Pollution Reports* 11:33
- [189] Martín-Lara MA, Blázquez G, Ronda A, Calero M. 2016. Kinetic study of the pyrolysis of pine cone shell through non-isothermal thermogravimetry: Effect of heavy metals incorporated by biosorption. *Renewable Energy* 96:613–624
- [190] Cai P, Fu J, Zhan M, Jiao W, Chen T, et al. 2022. Formation mechanism and influencing factors of dioxins during incineration of mineralized refuse. *Journal of Cleaner Production* 342:130762
- [191] Hu M, Guo K, Zhou H, Zhu W, Deng L, Dai L. 2024. Techno-economic assessment of swine manure biochar production in large-scale piggeries in China. *Energy* 308:133037
- [192] Struhs E, Mirkouei A, You Y, Mohajeri A. 2020. Techno-economic and environmental assessments for nutrient-rich biochar production from cattle manure: A case study in Idaho, USA. *Applied Energy* 279:115782
- [193] Sahoo K, Upadhyay A, Runge T, Bergman R, Puettmann M, et al. 2021. Life-cycle assessment and techno-economic analysis of biochar produced from forest residues using portable systems. *The International Journal of Life Cycle Assessment* 26:189–213
- [194] Nematian M, Keske C, Ng'ombe JN. 2021. A techno-economic analysis of biochar production and the bioeconomy for orchard biomass. *Waste Management* 135:467–477
- [195] Sessions J, Smith D, Trippie KM, Fried JS, Bailey JD, et al. 2019. Can biochar link forest restoration with commercial agriculture? *Biomass and Bioenergy* 123:175–185
- [196] Mukherjee A, Okolie JA, Niu C, Dalai AK. 2022. Techno – economic analysis of activated carbon production from spent coffee grounds: Comparative evaluation of different production routes. *Energy Conversion and Management: X* 14:100218
- [197] Varma VS, Parajuli R, Scott E, Canter T, Lim TT, et al. 2021. Dairy and swine manure management – challenges and perspectives for sustainable treatment technology. *Science of The Total Environment* 778:146319
- [198] Whalen JK, Thomas BW, Sharifi M. 2019. Novel practices and smart technologies to maximize the nitrogen fertilizer value of manure for crop production in cold humid temperate regions. In *Advances in Agronomy*, ed. Sparks DL. vol. 153. Cambridge: Academic Press. pp. 1–85 doi: [10.1016/bs.agron.2018.09.002](https://doi.org/10.1016/bs.agron.2018.09.002)
- [199] Jin R, Zhao C, Song Y, Qiu X, Li C, Zhao Y. 2023. Competitive adsorption of sulfamethoxazole and bisphenol A on magnetic biochar: Mechanism and site energy distribution. *Environmental Pollution* 329:121662



Copyright: © 2025 by the author(s). Published by Maximum Academic Press, Fayetteville, GA. This article is an open access article distributed under Creative Commons Attribution License (CC BY 4.0), visit <https://creativecommons.org/licenses/by/4.0/>.